Computation of scattering from clusters of spheres using the fast multipole method

Nail A. Gumerov and Ramani Duraiswami
Perceptual Interfaces and Reality Laboratory, Institute for Advanced Computer Studies, University of Maryland, College Park, Maryland 20742

(Received 23 June 2004; revised 5 November 2004; accepted for publication 1 December 2004)

A T-matrix based method of solution of the multiple scattering problem was presented by the authors [J. Acoust Soc. Am. **112**, 2688–2701 (2002)]. This method can be applied to the computation of relatively small problems, since the number of operations required grows with the number of spheres N as $O(N^3)$, and with the sixth power of the wave number. The use of iterative techniques accelerated using the fast multipole method (FMM) can accelerate this solution, as presented by Koc and Chew [J. Acoust. Soc. Am. **103**, 721–734 (1998)] originally. In this study we present a method that combines preconditioned Krylov subspace iterative techniques, FMM accelerated matrix vector products, a novel FMM-based preconditioner, and fast translation techniques that enable us to achieve an overall algorithm in which the cost of the matrix-vector multiplication grows with N as $O(N \log N)$ and with the third power of the wave number. We discuss the convergence of the iterative techniques, selection of the truncation number, errors in the solution, and other issues. The results of the solution of test problems obtained with the method for $N \sim 10^2 - 10^4$ for different wave numbers are presented. [DOI: 10.1121/1.1853017]

PACS numbers: 43.20.Fn Pages: 1744–1761

I. INTRODUCTION

Problems of acoustic and electromagnetic wave propagation through a medium consisting of the carrier fluid or solid and inclusions in the form of solid particles, droplets, and bubbles are of great practical and theoretical interest, and there are several approaches for the modeling of these. One approach is based on the development of continuum theories that treat a large system as a single complex medium with special properties that are obtained on the basis of spatial or other types of averaging (e.g., see Nigmatulin, 1990; Caflisch *et al.*, 1985). This approach is validated against experiments and has many strengths, such as a relative simplicity of the description, a clear relation to the physics, and the operation with quantities that can be measured. However, as with any theory, the continuum theories have some limits and restrictions that follow from basic assumptions. For example, the models normally are based on assumptions that the medium is acoustically homogeneous (Gumerov *et al.*, 1988; Duraiswami and Prosperetti, 1995). This means that the wavelengths should be much larger than the characteristic size a and distance d between the particles ($ka \ll 1$, $kd \ll 1$, where k is the wave number). While some assumptions can be relaxed, an accurate averaging procedure should take into account many real effects, and unavoidably introduces assumptions that permit one to link the description of the processes at the ''microlevel'' with the behavior of quantities at the ''macrolevel.''

Another approach is based on the direct computation of the acoustic field in the system at the level of particle sizes, based on fundamental governing equations applicable at the ''microlevel.'' While valid and free of many limitations of the continuum theory, this approach is computationally challenging. It is more or less obvious that there should be substantial efforts toward some theories that combine direct computations, stochastic and continuum medium approach to extend their limits, and, in fact, this is not a purpose of this paper. Here we are interested with a solution of some ''intermediate'' class of problems, when, on the one hand, the number of particles is large enough to make conclusions of a statistical nature, and, on the other hand, may be small compared to real systems.

The problems, which are out of the range of continuum theories, are related to the acoustic wavelengths, which are comparable with the size of the particles. This may include both ultrasound propagation in dispersed systems, or lower-frequency sound propagation in some environment with larger objects (e.g., fish). In this case the number of scatterers in the system can be, say, several thousands. Since in the present paper we are solving the problem for the three-dimensional (3D) Helmholtz equation, which also appears in electromagnetics, the method may also be applicable to the solution of problems in diffraction optics, x-ray scattering, and so on. In many situations the scatterers can be assumed to be spherical, and the boundary conditions on the scatterer have a strong influence on the results.

There exist several approaches to the solution of the multiple scattering problems, and the T-matrix method and its modifications are among these approaches (Waterman and Truell, 1961; Peterson and Strom, 1974; Varadan and Varadan, 1980; Wang and Chew, 1993; Mischenko *et al.*, 1996; Koc and Chew, 1998) and recently in our paper [Gumerov and Duraiswami, 2002; which in the sequel we will refer to as (GD02)]. A solution of the problem for spherical scatterers based on a multipole re-expansion technique was presented in (GD02). This solution is based on a representation of the scattered field for each sphere by a series of multipoles, the coefficients of which can be determined by applying the impedance boundary conditions cor-

responding to each sphere. This was achieved using reexpansion matrices, which enable one to find the expansion coefficients in a basis conveniently located at the center of an arbitrary scatterer. Since the series are infinite, we used truncation to keep only p^2 terms in the series, where p is a quantity termed the truncation number.

In (GD02) the computational complexity for solution of this problem for N scatterers is $O(p^6N^3)$. While we found that this method is reliable and fast for relatively small N and p, the solution of problems for a larger number of scatterers ($N \gtrsim 10^3$) or higher frequencies (since for convergence $p > ka$) with this method is computationally intractable.

Such computations are also known as ''brute-force'' method, and there exist several papers in electromagnetics and acoustics that present algorithms of lower complexity. For example, Wang and Chew (1993), present a generalized recursive aggregate T-matrix algorithm (RATMA), with complexity $O(p^2P^4N)$ (in our notation), where P^2 is the number of harmonics to expand the field of the aggregated scatterers. The latter quantity is related to the size of the computational domain, D_0, and $P \sim kD_0$. If we assume that the volume fraction of scatterers is constant, and so $D_0 \sim N^{1/3}a$, and since the truncation numbers can be estimated as $p \sim ka$, we can see that actually the RATMA scales as $O(p^6N^{7/3})$. The RATMA does not improve the sixth power in the complexity dependence on p. That is why the computations with this algorithm can be performed only for low p (i.e., low ka). For example, Wang and Chew (1993) presented computations of electromagnetic scattering problem for large enough $N=6859$, but for relatively low $kD_0<10$ (truncation numbers in these computations $p \leqslant 3$). In this context we should note that the accuracy of computations depends not only on the size of the domain or the size of scatterers (kD_0 and ka), but also on the interparticle distances, d/a. Even for $ka<1$, truncation numbers can be, say $p \sim 15$, for the relatively low accuracy of computations of 1%, in the case that the scatterers are nearly touching (see the discussion on truncation numbers later in this paper).

Another, rather obvious, idea to improve the ''brute-force'' method is to use iterative methods for a solution of the linear system. If N_{iter} is the number of iterations to achieve a required accuracy and each iteration requires one matrix-vector multiplication, which can be performed directly for $O(p^4N^2)$ operations, the total complexity of the algorithm will be $O(p^4N^2N_{\text{iter}})$. Comparing with the RATMA, we can see that for $N_{\text{iter}} \ll p^2N^{1/3}$, an iterative technique is faster.

A further improvement of the algorithm complexity comes from the acceleration of the matrix-vector multiplication. Currently two major techniques are known to reduce the complexity of solution from $O(N^2)$ to $O(N \log N)$ or $O(N)$ (if we assume that the truncation number does not depend on N): the Fast Fourier Transform (FFT) and the Fast Multipole Method (FMM).

The FFT cannot be applied if the scatterers are not located in a regular grid. However, this can be fixed by using translations from the scatterer locations to the regular grid, which is an idea of the FMMFFT (Koc and Chew, 1998). As originally introduced, the FMMFFT utilizes the diagonal forms of the translation operators and has complexity $O(p^4N+p^2N \log N)$. Recently some modifications of the FMMFFT, such as the FFTM (Ong *et al.*, 2004) appeared in the literature, which utilize different translation methods (recursively computed translation matrices) and have complexity $O(p^4N \log N)$.

The FMM was introduced in Greengard and Rokhlin (1987) for solution of the Laplace equation in two and three dimensions. Later, this method was intensively studied and extended to a solution of many other problems. Sangani and Mo (1996) applied it to multiparticle systems using the analog of the T-matrix idea for the case of Laplace and Stokes interactions of multiple particles via the FMM.

In the original work, functions were represented via a set of expansion coefficients over a local or multipole basis. The translation operators in this case appeared to be dense matrices converting one set of the expansion coefficients to the other. If the number of expansion coefficients is p^2, this results in $O(p^4)$ translation complexity and in $O(p^4N)$ overall complexity of the algorithm if p is the same for all the levels of hierarchical space subdivision. In the case of the Laplace equation, this results in a fast enough algorithm. However, for the Helmholtz equation for a given accuracy, the number of terms needed in the expansion grows with the largest length scale in the problem. Consequently, if we want to use the method as is, then for the Helmholtz equation instead of p^2 we should use P^2, which is the number of terms needed to represent the function at the coarsest level. For a uniform volume distribution of the scatterers with a constant volume fraction, we have $P \sim kD_0 \sim kaN^{1/3} \sim pN^{1/3}$, which results in $O(p^4N^{7/3})$ complexity. This is slower than $O(p^4N^2)$ required for direct matrix-vector multiplication, and so the FMM in its original form is not applicable to the scattering problem.

To reduce the cost of the FMM, an alternative function representation, via samples of the so-called ''signature function'' (also called the Herglotz wave function), was introduced by Rokhlin (1993). This representation gives rise to the diagonal forms of the translation operators. The number of samples is proportional to the number of harmonics in spectral representation, and here we can treat this quantity as p^2. The diagonal forms provide $O(p^2)$ translation complexity. If the original FMM using the diagonal forms is employed for a solution of the Helmholtz equations, we should use P^2 instead of p^2 that results in $O(P^2N)=O(p^2N^{5/3})$ complexity of the matrix-vector multiplication. As was suggested by Rokhlin, the way to overcome these large complexities in the FMM is to vary the size of the vectors representing functions from level to level.

The algorithm of this type based on the diagonal forms of the translation operators with interpolation/anterpolation procedures (MLFMA) is presented in Chew *et al.* (2001) and used for the acoustic scattering problems by Koc and Chew (1998). If the interpolation/anterpolation procedures are performed with complexity $O(M)$ for $O(M)$ samples of the signature function with the required accuracy, then a solution of the Helmholtz equation can be obtained for $O(p^2N)$ operations. The algorithm of Koc and Chew (1998), however, formally has complexity $O(p^4N)$, since it requires a conver-

sion of the function representation from the set of multipole expansion coefficients to samples of the signature function, and further accounting for near interactions is also estimated (by us) as $O(p^3N)$. Our computations show that for dense systems a computation of the near interactions can be several times more expensive than a computation of the farfield interactions.

In fact, the $O(p^4N)$ conversion is not a necessary step for the algorithm if it operates with the expansion coefficients and uses matrix translation operators. The complexity of such nondiagonalized operations can be reduced to $O(p^3)$ for p^2 expansion coefficients using rotational–coaxial translation decomposition, and this is sufficient to achieve $O(p^3N\log N)$ overall complexity of the matrix-vector multiplication for the volume distribution of scatterers. While this fact is simple and we provide its proof in this paper, it seems to have been overlooked in the previous publications, where one can find statements that only the diagonal forms of the translation operators provide algorithms scaled as $O(N)$ or $O(N\log N)$ for the Helmholtz equation. The benefits of operating in the space of expansion coefficients also include stability of the translations, which does not require interpolation/anterpolation or spherical filtering procedures that are necessary for the methods using diagonal forms and is an expensive part of it (Darve, 2000a; Chew *et al.*, 2001). Another benefit is the stability of computations for the cases of low *ka* and relatively large *p*.

While the paper of Koc and Chew (1998) presumably is the first that uses a combination of the T-matrix method and iterative techniques accelerated by the FMM and/or FFT for solution of acoustic scattering problems, several important issues still remain to be worked out. First, the iterative techniques presented in that paper are relatively standard, and their rate of convergence can be slow. As we found from our numerical experiments for systems of densely packed scatterers, N_{iter} at sufficiently large N may even grow as $O(N)$, which brings the total complexity of the FMM accelerated methods to $O(N^2)$ or $O(N^2\log N)$. One of the ways to treat this problem is to use properly designed preconditioners. In this paper we introduce for the first time the flexible generalized minimal residual method (FGMRES) with a right dense preconditioner, which can also be computed with the FMM/GMRES. Our results show that this can substantially speed up the algorithm, and experimental data on the complexity fit complexities $O(N^{1+\beta})$ with low β. Second, we establish both *a priori* error bounds and used an *a posteriori* error check of the solution to see how the error depends on the relative scatterer locations and the truncation numbers used. Third, as it was presented, the T-matrix could be arbitrary, but at the same time the application of the method to real problems of interest in computational acoustics was limited. In the present paper we apply the solution to problems that have been studied extensively in acoustics, of multiple scattering from spheres. To solve this problem, we exploited the multipole solution for the boundary value problem for spheres presented in (GD02) and used the explicit T matrices, which depend on the scatterer sizes, impedances, etc. This allows one to model and investigate various parametric dependencies, and, move the method to the solution of general practical acoustical problems. Finally, we used a variant of the FMM operating with expansion coefficients only, where the rectangularly truncated translation operators were computed using fast recursive algorithms and decompositions (Gumerov and Duraiswami, 2003). Numerical experiments show the performance and efficiency of our algorithm and support, that the matrix-vector multiplication is performed with $O(N)$ or $O(N\log N)$ complexity.

II. STATEMENT OF THE PROBLEM

The problem considered is that in (GD02), and is repeated here to establish the notation. Consider sound scattering by N spheres with radii $a_1,\ldots,a_N$ situated in $\mathbb{R}^3$. The coordinates of the centers of the spheres are denoted as $\mathbf{r}'_q=(x'_q,y'_q,z'_q)$, $q=1,...,N$. The scattering problem in the frequency domain is reduced to the solution of the Helmholtz equation for complex potential $\psi(\mathbf{r})$,

$$\nabla^2\psi+k^2\psi=0, \tag{1}$$

with the following general impedance boundary conditions on the surface S_q of the qth sphere:

$$\left(\frac{\partial\psi}{\partial n}+i\sigma_q\psi\right)\Big|_{S_q}=0, \quad q=1,...,N, \tag{2}$$

where k is the wave number and σ_q are complex admittances, and $i=\sqrt{-1}$. In the particular case of sound-hard surfaces ($\sigma_q=0$) we have the Neumann boundary conditions,

$$\partial\psi/\partial n|_{S_q}=0, \tag{3}$$

and in the case of sound soft surfaces ($\sigma_q=\infty$) we have the Dirichlet boundary conditions,

$$\psi|_{S_q}=0. \tag{4}$$

Usually the potential is represented in the form

$$\psi(\mathbf{r})=\psi_{\text{in}}(\mathbf{r})+\psi_{\text{scat}}(\mathbf{r}), \tag{5}$$

where $\psi_{\text{scat}}(\mathbf{r})$ is the potential of the scattered field. Far from the region occupied by spheres, the scattered field should satisfy the Sommerfeld radiation condition:

$$\lim_{r\to\infty} r\left(\frac{\partial\psi_{\text{scat}}}{\partial r}-ik\psi_{\text{scat}}\right)=0. \tag{6}$$

We must determine $\psi(\mathbf{r})$ or $\psi_{\text{scat}}(\mathbf{r})$ at any $\mathbf{r}$ on the surface of the spheres or outside them.

III. SOLUTION USING THE MULTIPOLE RE-EXPANSION METHOD

A. T matrix for a single scatterer

We first solve the scattering problem (1)–(6) for a single scatterer ($N=1$) in an arbitrary incident field. We assume that the incident field has no singularities in the domain inside the scatterer or on its boundary, and since it satisfies the Helmholtz equation it can be expanded near the center of this scatterer, $\mathbf{r}'_q$ ($q=1$), in the form

$$\psi_{\text{in}}(\mathbf{r})=\sum_{n=0}^{\infty}\sum_{m=-n}^{n}E_n^{(q)m}R_n^m(\mathbf{r}_q)=\mathbf{E}^{(q)}\cdot\mathbf{R}(\mathbf{r}_q),$$

$$\mathbf{r}_q=\mathbf{r}-\mathbf{r}_q'. \tag{7}$$

Here $E_n^{(q)m}$ are the expansion coefficients of the potential over the basis of the regular solutions $R_n^m(\mathbf{r}-\mathbf{r}_q')$ of the Helmholtz equation in the spherical coordinates $\mathbf{r}_q=(r_q,\theta_q,\varphi_q)$ connected with the center of the sphere:

$$R_n^m(\mathbf{r}_q)=j_n(kr_q)Y_n^m(\theta_q,\varphi_q),$$

$$\mathbf{r}_q=r_q(\sin\theta_q\cos\varphi_q,\sin\theta_q\sin\varphi_q,\cos\theta_q),$$

$$n=0,1,...,\quad m=-n,\ldots,n, \tag{8}$$

where $j_n(kr)$ are the spherical Bessel functions of the first kind and $Y_n^m(\theta,\varphi)$ are the orthonormal spherical harmonics:

$$Y_n^m(\theta,\varphi)=(-1)^m\sqrt{\frac{2n+1}{4\pi}\frac{(n-|m|)!}{(n+|m|)!}}P_n^{|m|}(\cos\theta)e^{im\varphi},$$

$$n=0,1,...,\quad m=-n,\ldots,n, \tag{9}$$

where $P_n^m(\mu)$ are the associated Legendre functions. Further, for compactness of notation, we use the following abbreviation to denote the sum represented by the product of two vectors: $\mathbf{A}=\{A_n^m\}$ and $\mathbf{B}=\{B_n^m\}$:

$$\mathbf{A}\cdot\mathbf{B}=\sum_{n=0}^{\infty}\sum_{m=-n}^{n}A_n^mB_n^m,\quad \mathbf{A}=\{A_n^m\},\quad \mathbf{B}=\{B_n^m\}. \tag{10}$$

The scattered field $\psi^{(q)}(\mathbf{r})=\psi_{\text{scat}}(\mathbf{r})$ can be represented in the form

$$\psi^{(q)}(\mathbf{r})=\sum_{n=0}^{\infty}\sum_{m=-n}^{n}A_n^{(q)m}S_n^m(\mathbf{r}_q)=\mathbf{A}^{(q)}\cdot\mathbf{S}(\mathbf{r}_q). \tag{11}$$

Here $A_n^{(q)m}$ are the expansion coefficients of the potential over the basis of the singular at $\mathbf{r}=\mathbf{r}_q'$ radiating solutions $S_n^m(\mathbf{r}-\mathbf{r}_q')$ of the Helmholtz equation:

$$S_n^m(\mathbf{r}_q)=h_n(kr_q)Y_n^m(\theta_q,\varphi_q),$$

$$n=0,1,...,\quad m=-n,\ldots,n, \tag{12}$$

where $h_n(kr)$ are the spherical Hankel functions of the first kind.

By "T matrix for scatterer q" we mean the matrix $\mathbf{T}^{(q)}$ with elements $T_{nn'}^{(q)mm'}$ that relates the expansion coefficients of the incident and scattered fields:

$$\mathbf{A}^{(q)}=\mathbf{T}^{(q)}\mathbf{E}^{(q)},$$

$$\left(A_n^{(q)m}=\sum_{n=0}^{\infty}\sum_{m'=-n'}^{n'}T_{nn'}^{(q)mm'}E_{n'}^{(q)m'},\right.$$

$$\left.n=0,1,...,\quad m=-n,\ldots,n\right). \tag{13}$$

In general, the T matrix can be determined for a scatterer of an arbitrary shape by a solution of the corresponding boundary value problem (1)–(6). For the case of spheres, this solution can be obtained analytically, as shown in (GD02). Based on this solution, the T matrix for a spherical scatterer of radius a_q and complex admittance σ_q is a diagonal matrix with elements

$$T_{nn'}^{(q)mm'}=-\frac{j_n'(ka_q)+(\sigma_q/k)j_n(ka_q)}{h_n'(ka_q)+(\sigma_q/k)h_n(ka_q)}\delta_{nn'}\delta_{mm'}, \tag{14}$$

where $n,\ n'=0,1,...;\ m=-n,\ldots,n;$ and $m'=-n',\ldots,n'$.

B. Decomposition of the scattered field

Due to the linearity of the problem, the scattered field can be represented in the form

$$\psi_{\text{scat}}(\mathbf{r})=\sum_{q=1}^{N}\psi^{(q)}(\mathbf{r}), \tag{15}$$

where $\psi^{(q)}(\mathbf{r})$ can loosely be thought of as the part of the scattered field introduced by the qth sphere, though, of course, it contains the influence of all the spheres. Each potential $\psi_q(\mathbf{r})$ is regular outside the qth sphere and satisfies the Sommerfeld radiation condition, so that it can be represented as prescribed by Eq. (11). In the vicinity of the qth scatterer we can write Eq. (15) as

$$\psi_{\text{scat}}(\mathbf{r})=\psi^{(q)}(\mathbf{r})+\phi^{(q)}(\mathbf{r}),$$

$$\phi^{(q)}(\mathbf{r})=\sum_{q'\neq q}\psi^{(q')}(\mathbf{r}),\quad q,q'=1,...,N. \tag{16}$$

The latter sum represents the function $\phi^{(q)}(\mathbf{r})$ that is regular in the part of the domain occupied by the qth scatterer and so can be represented as

$$\phi^{(q)}(\mathbf{r})=\mathbf{B}^{(q)}\cdot\mathbf{R}(\mathbf{r}_q), \tag{17}$$

where $\mathbf{B}^{(q)}=\{B_n^{(q)m}\}$ is a vector of expansion coefficients over the basis of regular spherical functions (8). These coefficients can be expressed via the coefficients $\mathbf{A}^{(q')}$, $q'=1,...,N,\ q'\neq q$ for all the scatterers, except of the qth scatterer, as

$$\mathbf{B}^{(q)}=\sum_{q'\neq q}(\mathbf{S}|\mathbf{R})(\mathbf{r}_{q'q}')\mathbf{A}^{(q')},$$

$$\mathbf{r}_{q'q}'=\mathbf{r}_q'-\mathbf{r}_{q'}',\quad q,q'=1,...,N, \tag{18}$$

where $(\mathbf{S}|\mathbf{R})(\mathbf{r}_{q'q}')$ is the re-expansion matrix with elements $(S|R)_{nn'}^{mm'}(\mathbf{r}_{q'q}')$ defined as the coefficients of expansion of the singular basis functions centered at $\mathbf{r}_{q'}'$ over the regular basis functions centered at $\mathbf{r}_q'$ (see Gumerov and Duraiswami, 2003),

$$S_{n'}^{m'}(\mathbf{r}_{q'})=\sum_{n=0}^{\infty}\sum_{m=-n}^{n}(S|R)_{nn'}^{mm'}(\mathbf{r}_{q'q}')R_n^m(\mathbf{r}_q),$$

$$q,q'=1,...,N,\quad q'\neq q. \tag{19}$$

Now, using Eqs. (5), (7), (16), (11), and (17), we can represent the total field near the qth scatterer in the form

$$\psi(\mathbf{r})=\mathbf{E}_{\text{eff}}^{(q)}\cdot\mathbf{R}(\mathbf{r}_q)+\mathbf{A}^{(q)}\cdot\mathbf{S}(\mathbf{r}_q),\quad \mathbf{E}_{\text{eff}}^{(q)}=\mathbf{E}^{(q)}+\mathbf{B}^{(q)}, \tag{20}$$

where we introduced the notation $\mathbf{E}_{\text{eff}}^{(q)}$ for the expansion coefficients of the ''effective'' incident field near the qth scatterer. Indeed, the first equation (20) shows that the multiple scattering problem is equivalent to a single scattering problem for the qth scatterer placed in the field, which is a superposition of the actual incident field and the fields scattered by the other scatterers. In this case the solution of the boundary value problem (1)–(6) for the qth scatterer is given by the T matrix, which relates the expansion coefficients $\mathbf{A}^{(q)}$ and $\mathbf{E}_{\text{eff}}^{(q)}$ as prescribed by Eq. (13). So we have

$$\mathbf{A}^{(q)}=\mathbf{T}^{(q)}(\mathbf{E}^{(q)}+\mathbf{B}^{(q)}), \quad q=1,...,N. \tag{21}$$

Now we can see that the system of equations (18) and (21) with respect to $\mathbf{A}^{(q)}$ and $\mathbf{B}^{(q)}$ is closed, as $\mathbf{T}^{(q)}$ and $\mathbf{E}^{(q)}$ are known (given). The coefficients $\mathbf{B}^{(q)}$ can be excluded to reduce the size of the system:

$$(\mathbf{T}^{(q)})^{-1}\mathbf{A}^{(q)}-\sum_{q'\neq q}(\mathbf{S}|\mathbf{R})(\mathbf{r}'_{q'q})\mathbf{A}^{(q')}=\mathbf{E}^{(q)}, \quad q=1,...,N. \tag{22}$$

This system also can be represented as a single equation,

$$\mathbf{LA}=\mathbf{E}, \tag{23}$$

where the vectors and matrices are stacked as

$$\mathbf{L}=\begin{pmatrix} (\mathbf{T}^{(1)})^{-1} & -(\mathbf{S}|\mathbf{R})(\mathbf{r}'_{21}) & \cdots & -(\mathbf{S}|\mathbf{R})(\mathbf{r}'_{N1}) \\ -(\mathbf{S}|\mathbf{R})(\mathbf{r}'_{12}) & (\mathbf{T}^{(2)})^{-1} & \cdots & -(\mathbf{S}|\mathbf{R})(\mathbf{r}'_{N2}) \\ \cdots & \cdots & \cdots & \cdots \\ -(\mathbf{S}|\mathbf{R})(\mathbf{r}'_{1N}) & -(\mathbf{S}|\mathbf{R})(\mathbf{r}'_{2N}) & \cdots & (\mathbf{T}^{(N)})^{-1} \end{pmatrix},$$

$$\mathbf{A}=\begin{pmatrix} \mathbf{A}^{(1)} \\ \mathbf{A}^{(2)} \\ \cdots \\ \mathbf{A}^{(N)} \end{pmatrix}, \quad \mathbf{E}=\begin{pmatrix} \mathbf{E}^{(1)} \\ \mathbf{E}^{(2)} \\ \cdots \\ \mathbf{E}^{(N)} \end{pmatrix}. \tag{24}$$

This system can be solved by appropriately truncating the infinite vectors to p^2 coefficients ($\mathbf{A}^{(q)}=\{A_n^{(q)m}\}$, $n=0,...,p-1$, $m=-n,\ldots,n$). The final linear system with Np^2 unknowns is the same as in (GD02) [where Eq. (22) was multiplied by matrix $\mathbf{T}^{(q)}$ for each q]. Therefore $O(N^3p^6)$ operations are required for a direct solution of this system. Using Eqs. (15) and (11) knowing all $\mathbf{A}^{(q)}$ enables the determination of $\psi_{\text{scat}}(\mathbf{r})$ everywhere in space. For the surface values of the potential and its normal derivatives simpler expressions can be used [see (GD02)].

IV. ITERATIVE METHODS

The first substantial reduction in complexity can be achieved by using iterative methods for solving the linear system. Assuming that each iteration involves one large dense matrix-vector multiplication of complexity $O(N^2p^4)$ and that the iterative process converges to the required accuracy in N_{iter} steps, we immediately obtain a computational complexity $O(N_{\text{iter}}N^2p^4)$ instead of $O(N^3p^6)$. For example, if $N\sim 100$, $p\sim 10$, and $N_{\text{iter}}\sim 10$, the savings could be of order 10^3 times. Of course convergence may be slow, but as long as $N_{\text{iter}}\ll Np^2$, the iterative procedure brings substantial savings. We note in this context that there exist methods (e.g., based on Krylov subspaces) that guarantee that an exact solution will be achieved in $N_{\text{iter}}\leqslant Np^2$ in exact arithmetics, while in practice the goal is to achieve this at much smaller N_{iter}.

Treating the multiple scattering problem as the solution of a dense linear system, we can employ different iterative methods starting from simple iterations to various versions of conjugate gradient, and Krylov subspace methods (see, e.g., Saad, 2003). Convergence of these methods can be improved by using well-designed preconditioners, block decompositions, etc.

The description and analysis of the entire area of iterative techniques is beyond the scope of this paper, and we refer the interested reader to the textbooks (Kelly, 1995; Saad, 2003). The use of a preconditioning matrix plays an important role, and the most efficient iterative schemes we used were based on the Flexible GMRES (FGMRES), which uses as the right preconditioner an approximate (GMRES) inverse of a matrix that approximates the system matrix $\mathbf{L}$ (24). We describe details of this iterative technique in the next section since it is related closely to the FMM-based matrix-vector product.

Any iteration method builds a sequence of approximations to the solution

$$\mathbf{A}_0^{(q)},\mathbf{A}_1^{(q)},\ldots; \quad \lim_{j\to\infty}\mathbf{A}_j^{(q)}=\mathbf{A}^{(q)}, \quad q=1,...,N, \tag{25}$$

where $\mathbf{A}_0^{(q)}$ is some initial guess, e.g.,

$$\mathbf{A}_0^{(q)}=\mathbf{T}^{(q)}\mathbf{E}^{(q)}, \quad q=1,...,N, \tag{26}$$

and stops when the convergence criterion is achieved. The convergence condition can be, e.g.,

$$\max_q\|\mathbf{A}_{j+1}^{(q)}-\mathbf{A}_j^{(q)}\|<\epsilon, \tag{27}$$

where $\|\ \|$ is some norm to measure the distance between two vectors (e.g., $\|\mathbf{A}\|=\max_{n,m}|A_n^m|$). Also, for each iteration it involves a computation of matrix vector product $\mathbf{LA}_j$ for a given input vector $\mathbf{A}_j$. Thus, the speed of an iterative method can be improved by reducing the number of iterations and speeding up the embedded matrix vector products.

If we turn to the equation to be solved (23), we can see from Eq. (24) that the matrix $\mathbf{L}$ can be decomposed as

$$\mathbf{L}=\mathbf{T}^{-1}-(\mathbf{S}|\mathbf{R}), \tag{28}$$

where $\mathbf{T}^{-1}$ is a diagonal matrix for spherical scatterers and block-diagonal otherwise, and $(\mathbf{S}|\mathbf{R})$ is the matrix consisting of the $(\mathbf{S}|\mathbf{R})(\mathbf{r}'_{qq'})$ blocks. Assuming that the product $\mathbf{T}^{-1}\mathbf{A}$ can be computed rapidly, we use the FMM to accelerate the computation of $\mathbf{B}=(\mathbf{S}|\mathbf{R})\mathbf{A}$, or

$$\mathbf{B}_j^{(q)}=\sum_{q'\neq q}(\mathbf{S}|\mathbf{R})(\mathbf{r}'_{q'q})\mathbf{A}_j^{(q')}, \quad q=1,...,N, \quad j=0,1,.... \tag{29}$$

V. FAST MULTIPOLE METHOD

The second substantial speed up of the solution can be obtained by accelerating the matrix-vector product (23) in the iterative methods via the multilevel Fast Multipole

Method (FMM). We refer the reader to details of the method in Greengard (1988) and for particulars of the method we used (Gumerov *et al.*, 2003). Below we describe the method used for the multiple scattering problems.

A. Data structures

The FMM operates with the spatial data organized in octrees. This means that the computational domain is the cube, or box, of size $D_0\times D_0\times D_0$ that encloses all the scatterers. We assign level 0 to this cube. Further, the computational domain is subdivided into eight smaller boxes $D_1\times D_1\times D_1$, each of size $D_1=0.5D_0$. This is referred to as level 1. Level 2 is obtained by the subdivision of boxes in level 1 by 8, and so on until some level $l_{\max}$, where there are $8^{l_{\max}}$ boxes of size $D_{l_{\max}}=2^{-l_{\max}}D_0$. To each box we assign some index (n,l), $n=0,...,8^l-1$, $l=0,...,l_{\max}$. Such a space partitioning generates a hierarchical data structure with "parent–children" relationships, where any box of level $l=0,...,l_{\max}-1$ can be considered as a "parent," with 8 children boxes obtained by its subdivsion. Neighbors of a box B are boxes at the same level, that share at least one boundary point with box B. Boxes that are not adjacent to the boundaries of the computational domain have 26 neighbors, which together with the box itself form the "neighborhood" of the box.

In the multiple scattering problem we say that scatterer q belongs to box (n,l) if the center $\mathbf{r}'_q$ of the smallest sphere enclosing the scatterer is located inside that box (for spherical scatters this sphere is simply its surface). Any box may intersect a scatterer, which does not belong to it (see Fig. 1). However, we require that the size of the smallest box (at the maximum level of space partitioning) is determined as below to ensure both the correctness of the FMM procedure and ensure the validity of the multipole re-expansions on the surfaces of neighboring scatterers. If the scatterers q and q' belong to two different boxes at the finest level with indices $(n_{q'},l_{\max})$ and $(n_{q'},l_{\max})$, which are not neighbors, then the field scattered by q' can be described by the local expansion of type (17) centered at the center of box $(n_q,l_{\max})$ in the domain occupied by the sphere surrounding the scatterer q. The maximum distance from the center of box $(n_{q'},l_{\max})$ to a point on the surface of scatterer q' is $D_{l_{\max}}\sqrt{3}/2+a_{\max}$, where $a_{\max}$ is the maximum possible size of the scatterer, $a_{\max}=\max(a_1,...,a_N)$. The minimum possible distance from the center of the box $(n_{q'},l_{\max})$ to a point on the surface of the qth scatterer is then $3D_{l_{\max}}/2-a_{\max}$. The requirement on the validity of expansions will be satisfied if $3D_{l_{\max}}/2-a_{\max}>D_{l_{\max}}\sqrt{3}/2+a_{\max}$, which yields the following condition:

$$D_{l_{\max}}>\frac{4}{3-\sqrt{3}}a_{\max}\approx 3.15a_{\max},$$

$$l_{\max}<\log_2\left(\frac{3-\sqrt{3}}{4}\frac{D_0}{a_{\max}}\right). \tag{30}$$

Note that this condition also ensures that the farfield reexpansion about the center of the box $(n_q,l_{\max})$ of the field scattered by scatterer q is valid at any point on the surface of the scatterer q'.

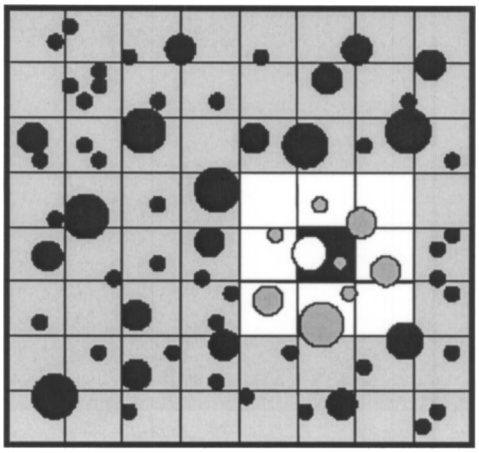

FIG. 1. Illustration of space partitioning and data structure for multiple scattering problem. The minimal spheres enclosing each scatterer are shown (so an actual scatterer of arbitrary shape is located inside the sphere). The white sphere belongs to the black box. The gray spheres are its neighbors. These are spheres which belong (in terms of their centers) to the E_2 neighborhood of the black box. The black spheres are the far spheres, they belong to the E_3 neighborhood of the black box (the centers are located outside the E_2 neighborhood). For a description of different neighborhoods see also Fig. 2.

A stronger limitation on $l_{\max}$ follows from formal requirements of the translation theory. Again, we can consider two closest boxes $(n_{q'},l_{\max})$ and $(n_q,l_{\max})$, which are not neighbors, and try to evaluate the effect of scatterer q' on q. The multipole series representing the potential of the scatterer q', whose center in the worst case is located at distance $D_{l_{\max}}\sqrt{3}/2$ from the center of the box $(n_{q'},l_{\max})$ should be translated first to the center of this box, then to the center of the box $(n_q,l_{\max})$, and finally to the center of scatterer q with a guarantee that the final local expansion is valid within the sphere of radius $a_{\max}$. This can be provided if $2D_{l_{\max}}>D_{l_{\max}}\sqrt{3}/2+D_{l_{\max}}\sqrt{3}/2+a_{\max}$, which is a condition that spheres of radii $D_{l_{\max}}\sqrt{3}/2$ and $D_{l_{\max}}\sqrt{3}/2+a_{\max}$ circumscribing the boxes $(n_{q'},l_{\max})$ and $(n_q,l_{\max})$, respectively, do not intersect ($2D_{l_{\max}}$ is the distance between the box centers). This condition can also be rewritten as

$$D_{l_{\max}}>\frac{1}{2-\sqrt{3}}a_{\max}\approx 3.73a_{\max},$$

$$l_{\max}<\log_2\left[(2-\sqrt{3})\frac{D_0}{a_{\max}}\right]. \tag{31}$$

A further limitation on $l_{\max}$ should be imposed, since we use truncated expansions. The truncation error is a function of the truncation number, which in turn depends on the distance between the center of the domain of local expansion and the closest point on the sphere surrounding the box containing the multipole, $b_{l_{\max}}=2D_{l_{\max}}-D_{l_{\max}}\sqrt{3}/2$. The dimensionless parameter,

$$\delta_{\min}=b_{l_{\max}}/(D_{l_{\max}}\sqrt{3}/2+a_{\max})>1, \tag{32}$$

then plays an important role for a selection of the truncation number (see the section below) ($p\to\infty$ for $\delta_{\min}\to 1$). If this parameter is specified, then we have the following modification for condition (31):

$$D_{l_{\max}} \geqslant \frac{2\delta_{\min}}{4-(1+\delta_{\min})\sqrt{3}}\, a_{\max},$$

$$l_{\max} \leqslant \log_2\left[\frac{4-(1+\delta_{\min})\sqrt{3}}{2\delta_{\min}}\,\frac{D_0}{a_{\max}}\right], \quad \delta_{\min}>1. \tag{33}$$

It can be seen that in any case $\delta_{\min}<4/\sqrt{3}-1\approx 1.31$. Note that in some test cases we found numerically that the algorithm may continue to perform satisfactorily when $l_{\max}$ exceeds the value prescribed by conditions (30)–(33).

B. Field decomposition

The field $\phi^{(q)}(\mathbf{r})$ [see Eq. (17)] due to the potentials centered at spheres other than the qth sphere can be decomposed into two parts:

$$\begin{aligned}&\phi^{(q)}(\mathbf{r})=\phi^{(q)}_{\text{near}}(\mathbf{r})+\phi^{(q)}_{\text{far}}(\mathbf{r}), \quad \mathbf{B}^{(q)}=\mathbf{B}^{(q)}_{\text{near}}+\mathbf{B}^{(q)}_{\text{far}},\\ &\phi^{(q)}_{\text{near}}(\mathbf{r})=\mathbf{B}^{(q)}_{\text{near}}\cdot\mathbf{R}(\mathbf{r}_q), \quad \phi^{(q)}_{\text{far}}(\mathbf{r})=\mathbf{B}^{(q)}_{\text{far}}\cdot\mathbf{R}(\mathbf{r}_q),\end{aligned} \tag{34}$$

where $\phi^{(q)}_{\text{near}}(\mathbf{r})$ is the field potential centered at the spheres that belong to the neighborhood $\Omega^{(q)}$ of the box containing the qth sphere at level $l_{\max}$, $\phi^{(q)}_{\text{far}}(\mathbf{r})$ is the field scattered by the other spheres, and $\mathbf{B}^{(q)}_{\text{near}}$ and $\mathbf{B}^{(q)}_{\text{far}}$ are the respective expansion coefficients in the basis $\mathbf{R}(\mathbf{r}_q)$. According to Eq. (18), these coefficients can be written in the form

$$\mathbf{B}^{(q)}_{\text{near}}=\sum_{\mathbf{r}_{q'}\in\Omega^{(q)},\ q'\neq q}(\mathbf{S}|\mathbf{R})(\mathbf{r}'_{q'q})\mathbf{A}^{(q')},$$

$$\mathbf{B}^{(q)}_{\text{far}}=\sum_{\mathbf{r}_{q'}\notin\Omega^{(q)}}(\mathbf{S}|\mathbf{R})(\mathbf{r}'_{q'q})\mathbf{A}^{(q')}. \tag{35}$$

In the iterative algorithm, the coefficients $\mathbf{A}^{(q)}$ are known from the previous iteration step, and the purpose is to determine $\mathbf{B}^{(q)}$ for the next iteration step [see Eq. (29)]. As there are not many scatterers in the neighborhood of the qth sphere, the coefficients $\mathbf{B}^{(q)}_{\text{near}}$ can be computed directly using the first equation in (35). The major computational expense comes from the second sum. To compute $\mathbf{B}^{(q)}_{\text{far}}$ we use the FMM, as described in the next section. Based on a given set of coefficients $\{\mathbf{A}^{(q)}\}$, the FMM provides coefficients $\mathbf{D}^{(q)}$ of the farfield expansion near the center of the box at the finest level, containing the qth scatterer, $\mathbf{r}^{(q)}_*$:

$$\phi^{(q)}_{\text{far}}(\mathbf{r})=\mathbf{D}^{(q)}\cdot\mathbf{R}(\mathbf{r}-\mathbf{r}^{(q)}_*), \quad q=1,...,N. \tag{36}$$

To get $\mathbf{B}^{(q)}_{\text{far}}$, which are the coefficients for expansion about the center of the qth sphere we need to translate this expansion to the proper center. This can be done by using the local-to-local translation operator, or by applying the $(\mathbf{R}|\mathbf{R})$ re-expansion matrix to coefficients $\mathbf{D}^{(q)}$:

$$\mathbf{B}^{(q)}_{\text{far}}=(\mathbf{R}|\mathbf{R})(\mathbf{r}'_q-\mathbf{r}^{(q)}_*)\mathbf{D}^{(q)}, \quad q=1,...,N. \tag{37}$$

Here the $(\mathbf{R}|\mathbf{R})$ re-expansion matrix has entries $(R|R)^{mm'}_{nn'}$ that are the expansion coefficients of the regular basis function over the same type of basis, whose center is shifted:

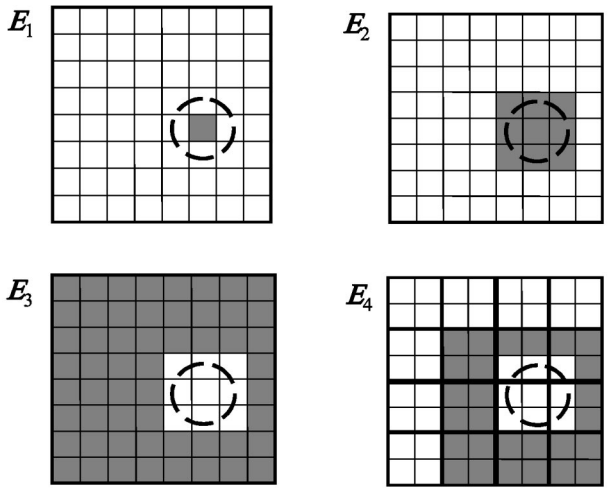

FIG. 2. The domains used for the construction of a hierarchical re-expansion procedure in FMM (shown in projection to a plane). A circle separates the box for which domains are drawn.

$$R^{m'}_{n'}(\mathbf{r}-\mathbf{r}^{(q)}_*)=\sum_{n=0}^{\infty}\sum_{m=-n}^{n}(R|R)^{mm'}_{nn'}(\mathbf{r}'_q-\mathbf{r}^{(q)}_*)R^m_n(\mathbf{r}_q),$$
$$q=1,...,N, \quad n'=0,1,..., \quad m'=-n',...,n'. \tag{38}$$

C. Details of the fast multipole method

In the FMM we introduce the following hierarchical domains, associated with each level of space subdivision: $E_1(n,l)$, the set of points located inside box (n,l); $E_2(n,l)$, the set of points located inside the neighborhood of box (n,l); $E_3(n,l)$, the set of points located in the computational domain, which are outside the neighborhood of box (n,l) [this domain is complementary to $E_2(n,l)$], and $E_4(n,l)$, the set of points located in domain $E_2(\text{Parent}(n),l-1)$, but outside domain $E_2(n,l)$. For boxes, whose parents are not adjacent to the boundaries of the computational domain, $E_4(n,l)$, consists of 189 boxes of level l. These domains are shown in Fig. 2. We associate fields $\psi^{(n,l)}_j(\mathbf{r})$ with every domain $E_j(n,l)$, $j=1,...,4$. These are fields scattered by all the spheres, which belong to the respective domains. We also associate truncation numbers $p_2,\ldots,p_{l_{\max}}$ with each level of subdivision $l=2,...,l_{\max}$. The selection of these truncation numbers is based on the error analysis and is discussed later. The algorithm consists of two major parts. In the first part we set up the hierarchical data structure, based on the location and sizes of the scatterers. This step need be performed only once for a given scatterer configuration, and is not repeated during the iterative process. The second part consists of the upward pass and the downward pass, followed by the final summation step, which is described by Eqs. (35) and (37), leads to a determination of the expansion coefficients $\mathbf{B}^{(q)}$, $q=1,...,N$.

1. Upward pass

The purpose of the upward pass is to determine coefficients $\mathbf{C}^{(n,l)}$ of expansion for all functions $\psi_1^{(n,l)}(\mathbf{r})$ over the bases of the S functions centered at the box centers $\mathbf{r}_*^{(n,l)}$:

$$\psi_1^{(n,l)}(\mathbf{r})=\mathbf{C}^{(n,l)}\cdot\mathbf{S}(\mathbf{r}-\mathbf{r}_*^{(n,l)}),\quad l=2,...,l_{\max},$$
$$\forall n,\quad \mathbf{r}'_q\in E_1(n,l),\quad q=1,...,N. \tag{39}$$

Here the length of the truncated coefficient vectors $\mathbf{C}^{(n,l)}$ and, respectively, the basis functions $\mathbf{S}(\mathbf{r}-\mathbf{r}_*^{(n,l)})$ depends on the level l and is of length p_l^2. To build the coefficients we apply the multipole-to-multipole, or the $(\mathbf{S}|\mathbf{S})$ translation operator, which can be thought of as a rectangularly truncated matrix with entries $(S|S)_{nn'}^{mm'}$, defined as re-expansion coefficients for the S functions:

$$S_{n'}^{m'}(\mathbf{r}+\mathbf{t})=\sum_{n=0}^{\infty}\sum_{m=-n}^{n}(S|S)_{nn'}^{mm'}(\mathbf{t})S_n^m(\mathbf{r}),$$
$$n'=0,1,...,\quad m'=-n',...,n', \tag{40}$$

where $\mathbf{t}$ is the translation vector determined by the location of the expansion centers. Note that for the Helmholtz equation we have $(\mathbf{S}|\mathbf{S})(\mathbf{t})=(\mathbf{R}|\mathbf{R})(\mathbf{t})$.

- Step 1. For each scatterer determine the coefficients of the S expansion centered at the center of the box $\mathbf{r}_*^{(q)}=\mathbf{r}_*^{(n,l_{\max})}$ at the finest level, $(n,l_{\max})$, to which this scatterer belongs using the multipole-to-multipole $S|S$ translation of the coefficients $\mathbf{A}^{(q)}$ to the center of this box:

$$\tilde{\mathbf{C}}^{(q)}=(\mathbf{S}|\mathbf{S})(\mathbf{r}_*^{(q)}-\mathbf{r}'_q)\mathbf{A}^{(q)},\quad q=1,...,N,$$
$$\mathbf{r}'_q,\mathbf{r}_*^{(q)}\in E_1(n,l_{\max}). \tag{41}$$

This step of the algorithm provides a representation of the scattered field for the qth scatterer (11) about the center of the box to which it belongs:

$$\psi^{(q)}(\mathbf{r})=\mathbf{A}^{(q)}\cdot\mathbf{S}(\mathbf{r}_q)=\tilde{\mathbf{C}}^{(q)}\cdot\mathbf{S}(\mathbf{r}-\mathbf{r}_*^{(q)}). \tag{42}$$

Note that the length of truncated vectors $\mathbf{A}^{(q)}$ is p^2, while the length of the truncated vectors $\tilde{\mathbf{C}}^{(q)}$ is $p_{l_{\max}}^2$. These lengths can be the same or different. We discuss this issue later.

Step 2. Consolidate all the expansions at the finest level, to obtain the expansion coefficients $\mathbf{C}^{(n,l_{\max})}$ of functions $\psi_1^{(n,l_{\max})}(\mathbf{r})$ over the S basis:

$$\mathbf{C}^{(n,l_{\max})}=\sum_{\mathbf{r}_*^{(q)}\in E_1(n,l_{\max})}\tilde{\mathbf{C}}^{(q)},\quad \mathbf{r}_*^{(n,l_{\max})}=\mathbf{r}_*^{(q)}. \tag{43}$$

Step 3. For $l=l_{\max}-1,...,2$, recursively obtain expansion coefficients $\mathbf{C}^{(n,l)}$ for all other functions $\psi_1^{(n,l)}(\mathbf{r})$ over the S basis using the multipole-to-multipole translation operators from the centers of children boxes containing the scatterers, $\mathbf{r}_*^{(n',l+1)}$, to the center of their parent box, $\mathbf{r}_*^{(n,l)}$, and the consolidation of the coefficients:

$$\mathbf{C}^{(n,l)}=\sum_{n'\in\text{Children}(n,l)}(\mathbf{S}|\mathbf{S})(\mathbf{r}_*^{(n,l)}-\mathbf{r}_*^{(n',l+1)})\mathbf{C}^{(n',l+1)}. \tag{44}$$

Here Children(n,l) denotes the set of children boxes for box (n,l). These boxes are of a smaller size than (n,l) and located at the level $l+1$.

2. Downward pass

The purpose of the downward pass is to determine coefficients $\mathbf{D}^{(n,l)}$ of expansion for all functions $\psi_3^{(n,l)}(\mathbf{r})$ over the bases of the R functions centered at $\mathbf{r}_*^{(n,l)}$:

$$\psi_3^{(n,l)}(\mathbf{r})=\mathbf{D}^{(n,l)}\cdot\mathbf{R}(\mathbf{r}-\mathbf{r}_*^{(n,l)}),\quad l=2,...,l_{\max},$$
$$\forall n,\quad \mathbf{r}'_q\in E_1(n,l),\quad q=1,...,N. \tag{45}$$

Here the length of truncated coefficient vectors $\mathbf{D}^{(n,l)}$ and, respectively, the basis $\mathbf{R}(\mathbf{r}-\mathbf{r}_*^{(n,l)})$ depends on the level l and is p_l^2. To build them we apply the multipole-to-local and local-to-local, or the $(\mathbf{S}|\mathbf{R})$ and $(\mathbf{R}|\mathbf{R})$ translation operators, which can be thought of as square and rectangularly truncated matrices, respectively, since the $(\mathbf{S}|\mathbf{R})$ translation is applied for boxes at the same level, while the $(\mathbf{R}|\mathbf{R})$ translation is used to translate coefficients from a lower level to a higher level. In the process we also determine coefficients $\tilde{\mathbf{D}}^{(n,l)}$ of expansion for potential $\psi_4^{(n,l)}(\mathbf{r})$ over the local bases:

$$\psi_4^{(n,l)}(\mathbf{r})=\tilde{\mathbf{D}}^{(n,l)}\cdot\mathbf{R}(\mathbf{r}-\mathbf{r}_*^{(n,l)}),\quad l=2,...,l_{\max},$$
$$\forall n,\quad \mathbf{r}'_q\in E_1(n,l),\quad q=1,...,N. \tag{46}$$

We need to do this in terms of organization of the hierarchical procedure, which is based on the following property of the domains $E_3(n,l)$ and $E_4(n,l)$ (see Fig. 2):

$$E_3(n,l)=E_3(n',l-1)\cup E_4(n,l),\quad n'=\text{Parent}(n). \tag{47}$$

This results in

$$\psi_3^{(n,l)}(\mathbf{r})=\psi_3^{(n',l-1)}(\mathbf{r})+\psi_4^{(n,l)}(\mathbf{r}),\quad n'=\text{Parent}(n), \tag{48}$$

and enables recursion with respect to the levels of the octree.

- Step 1. (This step and step 2 of the downward pass are performed recursively for $l=2,...,l_{\max}$.) Obtain coefficients $\tilde{\mathbf{D}}^{(n,l)}$ for all boxes containing the scatterers. We obtain these coefficients by the multipole-to-local translations of respective coefficients $\mathbf{C}^{(n',l)}$, followed by the consolidation of the expansions:

$$\tilde{\mathbf{D}}^{(n,l)}=\sum_{\mathbf{r}_*^{(n',l)}\in E_4(n,l)}(\mathbf{S}|\mathbf{R})(\mathbf{r}_*^{(n,l)}-\mathbf{r}_*^{(n',l)})\mathbf{C}^{(n',l)},$$
$$\forall n,n',\quad \mathbf{r}'_q\in E_1(n,l),\quad \mathbf{r}'_{q'}\in E_1(n',l),\quad q,q'=1,...,N. \tag{49}$$

Step 2. At level $l=2$ we have $E_3(n,2)=E_4(n,2)$, which results in $\mathbf{D}^{(n,2)}=\tilde{\mathbf{D}}^{(n,2)}$. For levels $l=3,...,l_{\max}$ we have, from Eq. (48),

$$\mathbf{D}^{(n,l)}=(\mathbf{R}|\mathbf{R})(\mathbf{r}_*^{(n,l)}-\mathbf{r}_*^{(n',l-1)})\mathbf{D}^{(n',l-1)}+\tilde{\mathbf{D}}^{(n,l)}, \tag{50}$$

$n'=\text{Parent}(n), \quad l=2,...,l_{\max}, \quad \forall n, \quad \mathbf{r}'_q \in E_1(n,l),$

$q=1,...,N.$

3. Final summation

The final summation step results in a determination of the scattered field at the current iteration, since the domains $E_3(n,l)$ and $E_2(n,l)$ are complementary. This step of the usual FMM procedure is skipped here, since all we need are the expansion coefficients at the finest level $\mathbf{D}^{(q)}=\mathbf{D}^{(n,l_{\max})}$, $\mathbf{r}'_q \in E_1(n,l_{\max})$, $q=1,...,N$. Equation (37) then provides coefficients $\mathbf{B}^{(q)}_{\text{far}}$.

D. Truncation numbers

To apply the algorithm we need to specify the truncation numbers p for the coefficients $\{\mathbf{A}^{(q)}\}$ and truncation numbers $p_2,\ldots,p_{l_{\max}}$. Their selection depends on the acceptable error of computations, which is determined by the rate of convergence of the series being truncated. Consider first the selection of p.

The series under consideration converge absolutely and uniformly only for $p \geqslant ka$. For relatively low ka ($ka \lesssim 10$), one can select p as

$$p=[ka]+p_0(ka,\epsilon,\delta), \quad p_0 \geqslant 1, \quad \delta=b/a \geqslant 1, \quad \epsilon>0, \tag{51}$$

where p_0 depends on the prescribed accuracy ϵ and the distance b between the center of the scatterer and the closest point on the surface of the closest scatter. While there are some theories for the expansion errors (e.g., Koc *et al.*, 1999; Darve, 2000b), they usually deal with the error of expansion of a single source. We suggest the evaluation of p_0 based on error maps (or their approximations) obtained as a solution of the scattering problem for two spheres placed in the field of the plane incident wave, $\psi_{\text{in}}(\mathbf{r})=e^{i\mathbf{k}\cdot\mathbf{r}}$. This problem can be solved very rapidly based on direct matrix inversion for coaxial spheres (GD02), where the parameters p_0, ka, and δ can be varied within the range under consideration, while the error of the solution ϵ can be determined *a posteriori*, as the error in boundary conditions.

Indeed, we note that since any radiating basis function satisfies the Helmholtz equation, the expansion truncated with an arbitrary p will satisfy the Helmholtz equation and radiation condition (6). So the only equation that is not satisfied exactly by the approximate solution is the boundary condition (2). Once an approximate solution is computed, i.e., the expansion coefficients $\{\mathbf{A}^{(q)}\}$ are found, we can compute the normal derivative on the surface for any scatterer using the differentiation theorem for the spherical basis functions in an arbitrary direction specified by the unit vector $\mathbf{n}=(n_x,n_y,n_z)$ (Gumerov and Duraiswami, 2003):

$$\begin{aligned}\frac{1}{k}\mathbf{n}\cdot\nabla S_n^m(\mathbf{r}) &= \frac{1}{2}(n_x-in_y)[b_{n+1}^{-m-1}S_{n+1}^{m+1}(\mathbf{r})-b_n^m S_{n-1}^{m+1}(\mathbf{r})] \\ &+ \frac{1}{2}(n_x+in_y)[b_{n+1}^{m-1}S_{n+1}^{m-1}(\mathbf{r})-b_n^{-m}S_{n-1}^{m-1}(\mathbf{r})] \\ &+ n_z[a_{n-1}^m S_{n-1}^m(\mathbf{r})-a_n^m S_{n+1}^m(\mathbf{r})],\end{aligned} \tag{52}$$

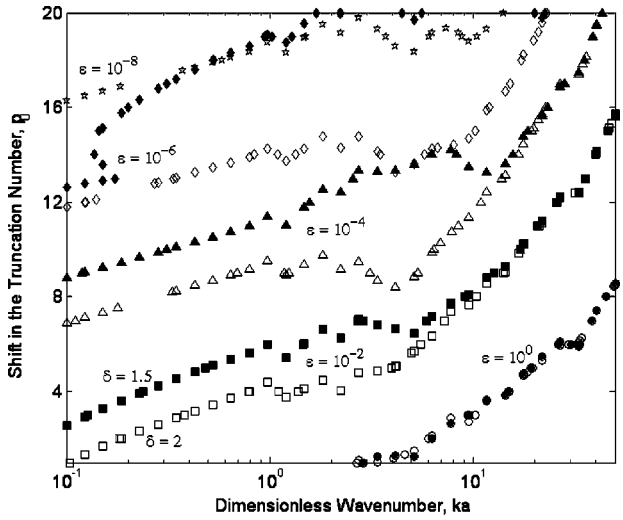

FIG. 3. Dependences of the shift in the truncation number, p_0, defined by Eq. (51) on the dimensionless wave number ka for two sound-hard spheres of equal size. The curves are computed to provide the error $\epsilon^{(bc)}$ in boundary conditions shown near the curves. Two sets of curves marked by the filled and empty symbols correspond to different distances between the spheres (δ=1.5 and δ=2, respectively).

where the coefficients a_n and b_n are specified by Eqs. (62) and (63). Therefore, as the truncated solution is computed, the left-hand side of Eq. (2) can be determined, and there are no additional errors for derivative computation or approximation. If we sample the surface with M points, we can then compute the following errors in boundary conditions:

$$\epsilon_m^{(bc)}=\frac{M|\Delta_{bc}(\mathbf{y}_m)|}{[\Sigma_m|\psi|_{S_q}(\mathbf{y}_m)|^2]^{1/2}}, \quad \epsilon^{(bc)}=\max_m \epsilon_m^{(bc)},$$

$$\Delta_{bc}(\mathbf{y}_m)=a_q\left(\frac{\partial\psi}{\partial n}(\mathbf{y}_m)+i\sigma_q\psi(\mathbf{y}_m)\Big|_{S_q}\right), \quad m=1,...,M. \tag{53}$$

Figure 3 illustrates dependencies $p_0(ka,\epsilon^{(bc)},\delta)$ for two fixed values of δ and a range of ka. The spheres are sound-hard, $\sigma_q=0$, $q=1,2$. Here for each curve $\epsilon^{(bc)}$ is fixed (p_0 is not an integer due to interpolation). $\epsilon^{(bc)}$ was computed according to Eq. (53), where each sphere was sampled with 181 equispaced points with respect to the spherical polar angle θ. For the low-frequency region, $ka \lesssim 1$ and $\epsilon^{(bc)} \gtrsim 10^{-4}$, we have $p_0 \sim p_{00}(\epsilon,\delta)+\log(ka)$, which in the semilogarithmic coordinates is a linear dependence. For higher frequencies, $ka \gg 1$, we have $p_0 \sim (ka)^\nu$, where theoretically $\nu=1/3$ and that is pretty close to our computations. The dependence on δ in this range is rather weak (when δ is not very close to unity), while for lower frequencies the truncation number substantially depends on this parameter. Figure 4 illustrates dependencies $p_0(ka,\epsilon^{(bc)},\delta)$ for fixed $ka=1$ and varying δ. It is seen that if the spheres are very close to each other ($\delta \sim 1$), the truncation number should be high to provide small errors. However, if it is sufficient to compute a solution with, say, $\sim$1% of relative error, these computations can be achieved with $p_0 \sim 10$, even when the spheres touch each other.

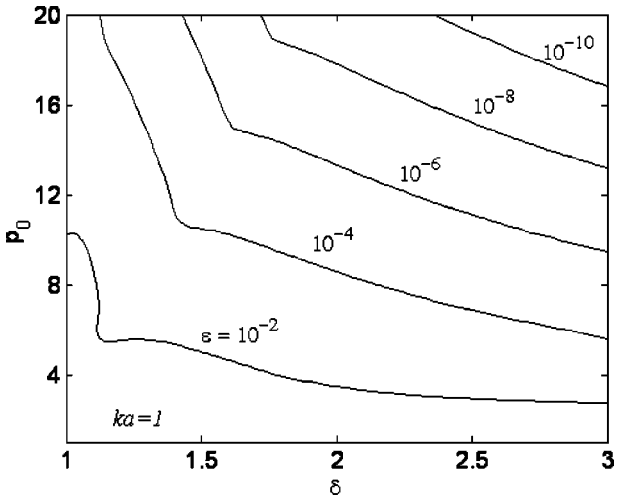

FIG. 4. Dependences of the shift in the truncation number, p_0, defined by Eq. (51) on the dimensionless parameter δ characterizing the distance between the spheres for two sound-hard spheres of equal size. The curves are computed to provide the error $\epsilon^{(bc)}$ in boundary conditions shown near the curves.

For larger ka the truncation number can be selected based on the high-frequency asymptotics of the spherical Bessel functions (e.g., see Chew *et al.*, 2001):

$$p = P(ka, \epsilon) = ka + \frac{1}{2}\left(3 \ln \frac{1}{\epsilon}\right)^{2/3} (ka)^{1/3}. \tag{54}$$

In this equation the truncation number does not depend on δ, while such a dependence can be introduced. Equation (54) is qualitatively consistent with the behavior of the error observed in computations where δ is not very close to 1. To relate it to the actual error observed for a solution of the two sphere scattering problem one should relate ϵ to $\epsilon^{(bc)}$, and we found that for the range plotted in Fig. 3 one can set $\epsilon \sim 10^{-2}\epsilon^{(bc)}$ to fit results for $ka > 1$.

Similar formulas can be applied for a computation of the truncation numbers used in the FMM, in which case we need to specify what we mean by a and δ here. The parameter a can be selected as the radius of the smallest sphere that encloses the box of level l plus $a_{\max}$ and δ formally is limited by the value $\delta < 1.31$ (see the discussion on $l_{\max}$ previously, while a more accurate analysis is required here, since the "worst case" analysis usually substantially overestimates actual errors). Since the size of this box is $D_l = 2^{-l} D_0$, one can set

$$a_l = 2^{-l-1} 3^{1/2} D_0 + a_{\max}, \quad p_l = P(ka_l, \epsilon). \tag{55}$$

In computations we used this formula for automatically setting the level-dependent truncation numbers with function $P(ka, \epsilon)$ specified by Eq. (54), where ϵ was some prescribed error. In computations we also performed an *a posteriori* actual error check using Eq. (53), which is valid for an arbitrary number of spheres.

We note also that for the present problem, when the number of scatterers can be large, and so for fixed ka and the volume fraction of scatterers we have $D_0 \sim N^{1/3} a$, truncation numbers p_l used in the FMM can be substantially larger than p. In other words, if the wavelength is comparable with the size of the scatterer, then the size of the computational domain is much larger than the wavelength for large N.

We can note that in the case when the spheres are close or may touch each other, p can be larger than p_l to provide the required accuracy. To avoid unnecessary computations in this case, translations for the farfield expansions at the finest level can be made to obtain only $p_{l_{\max}}^2$ terms, since terms of degree n corresponding to $p_{l_{\max}} \leqslant n < p$ are due to the influence of close neighbors. Moreover, in computations of the near field, we can subdivide the set of neighbor spheres into two sets: those that are closer than some prescribed b_* (or δ_*), for which the interaction should be computed using all p^2 terms, and the other neighbors, whose interactions with the given sphere can be efficiently computed using only $p_{l_{\max}}^2$ terms. We found numerically that these tricks may bring substantial savings in computational time, while almost not affecting the accuracy of the procedure.

E. Complexity estimates

In the FMM, translations occur between two subsequent levels l and $l+1$ (for the local-to-local or multipole-to-multipole translations) or on the same level l (for the multipole-to-local translations). Since the number of coefficients representing the potential for each box at level l is p_l^2 and $p_{l+1}^2 \sim p_l^2$, we can estimate the complexity of a single translation associated with level l as $O(p_l^{2\nu})$, where $\nu \geqslant 1$ is some parameter, that we call the "translation exponent." For example, if the translation is performed by multiplication of the translation matrix by the vector of coefficients, the complexity of the translation will be $O(p_l^4)$, in which case $\nu = 2$.

To evaluate the number of operations required for all translations, we assume that the scatterers are distributed more or less evenly in space, and so all 8^l boxes at level l contain some scatterers. The maximum number of translations associated with any box at level l is finite (8 multipole-to-multipole translations in the upward pass, 8 local-to-local translations in the downward pass, and 189 multipole-to-local translations in the downward pass). This shows that the translation cost associated with each box at level l is $O(p_l^{2\nu})$ (with a large asymptotic constant). Therefore the total number of translations can be evaluated as

$$N_{\text{trans}} = O\left(\sum_{l=2}^{l_{\max}} p_l^{2\nu} 8^l\right). \tag{56}$$

From Eqs. (54) and (55) we can majorate the dependence of p_l on l with function $p_l = \beta k D_0 2^{-l}$, where β is some constant. Substituting this into Eq. (56), we obtain

$$N_{\text{trans}} = (kD_0)^{2\nu} O\left(\sum_{l=2}^{l_{\max}} 2^{(3-2\nu)l}\right). \tag{57}$$

Three qualitatively different cases can be identified now. The first case, $\nu < 1.5$, corresponds to "fast translations." In this case we have $N_{\text{trans}} \sim (kD_0)^{2\nu} 2^{(3-2\nu) l_{\max}}$. Assuming that $D_0 \sim N^{1/3} a$, so $kD_0 \sim N^{1/3} ka \sim N^{1/3} p$ and $2^{3 l_{\max}} \sim N$, we can see that $N_{\text{trans}} \sim p^{2\nu} N$. So the algorithm scales as $O(p^{2\nu} N)$, with p taken for the truncation of coefficients $\{\mathbf{A}^{(q)}\}$ [see Eqs. (51) and (54)]. The second case, $\nu = 1.5$, corresponds to

the ''critically fast translations,'' and this value of ν can be called a ''critical translation exponent.'' We have then, using the same assumptions as for the first case, $N_{\text{trans}} \sim (kD_0)^3 l_{\max} \sim p^3 N \log N$, or complexity $O(p^3 N \log N)$. Finally, we have the case of ''slow translations,'' $\nu > 1.5$. Here $N_{\text{trans}} \sim (kD_0)^{2\nu} \sim p^{2\nu} N^{2\nu/3}$. So the FMM in this case scales as $O(p^{2\nu} N^{2\nu/3})$, or superlinearly with N, $2\nu/3 > 1$. It is interesting to note that in the first case the major number of translation operations are performed at the finest level of space partitioning $l_{\max}$, in the second case the number of operations for each level is approximately the same, while in the third case the major complexity comes from operations at the coarsest level $l=2$. So two competing effects, the reduction of the number of boxes, and an increase of the truncation numbers compensate each other in the ''critical'' case. To provide an algorithm that scales as $O(N \log N)$, one should use at least an $O(p^3)$ translation method.

Note that the theoretically minimum translation exponent is $\nu=1$ (one operation per one expansion coefficient). This value is also ''critical'' for two-dimensional problems, and for three-dimensional problems, where the scatterers are distributed over some surface. The later case also applies to the boundary element methods. For these cases to have an $O(N \log N)$ complexity FMM algorithm with a variable truncation number, one should employ the theoretically fastest translation methods.

Finally, we note that the total complexity of the method consists of the complexity of translations plus complexity of generation of function representations for each box at the finest level, the complexity of evaluation of function representations, and the final summation. In the present paper all procedures have complexity $O(p^3)$. Taking into account that such operations should be performed for each point, the total complexity of the present algorithm will be $N_{\text{oper}} = O(p^3 N) + O(p^3 N \log N) = O(p^3 N \log N)$.

In the paper of Koc and Chew (1998), the diagonal forms of the translation operators obtained by Rokhlin (1993) are used. Formally, the complexity of these translation methods can be evaluated as $O(p^2)$, while their implementation requires additional procedures, such as interpolation and anterpolation (e.g., see Darve, 2000a; Chew *et al.*, 2001), or the filtering of spherical harmonics. These procedures can be much more expensive than the translation itself [e.g., K-point Lagrange interpolation, the complexity can be evaluated as Kp^2, and for $K \sim p$ this results in $O(p^3)$ complexity], while they can be efficient for higher frequencies. In any case, if we assume that the complexity of the translation method is $O(p^2)$ ($\nu=1$) we obtain $N_{\text{trans}} \sim O(p^2 N)$. However, higher complexity comes from the initial and final steps of the algorithm. To use the diagonal forms we need to convert the representation based on expansion coefficients to that based on samples of the signature function over the sphere. A bandlimited function with p^2 coefficients can be represented by $O(p^2)$ samples, and the conversion of one representation to the other using a direct integral evaluation (as did Koc and Chew) requires $O(p^4)$ operations. The same relates to the final evaluation step, where we should convert function representation from the samples of the signature function to the expansion coefficients. So the total complexity of the Koc and Chew algorithm can be evaluated as $O(p^4 N) + O(p^2 N) = O(p^4 N)$. There may be some possibilities to improve the complexity of the Koc and Chew algorithm, e.g., if a fast Legendre transform were available (an item of current research). We note that formally the complexities of the Koc and Chew method and the present method are the same for $p \sim \log N$, while, in practice, the quality of implementation, which influences the asymptotic constants, can reduce the execution time of the algorithm several times and factors of type $\log N$ in the range of N considered in this paper are unimportant, except from a theoretical point of view.

F. Translation method

For the present class of problems $O(p^3)$-translation methods based on the use of the re-expansion matrices can be employed, as they provide a transparent link to the coefficients of the expansions.

The translation method based on a direct computation of the re-expansion matrices $(\mathbf{E}|\mathbf{F})(\mathbf{t})$, where $(\mathbf{E}|\mathbf{F})$ can be any combination of letters **S** and **R**, followed by their multiplication by the vectors of expansion coefficients has complexity $O(p^4)$. This is the lowest complexity that one can expect, even using recursive procedures for the computation of matrix elements, since the matrix is dense. To achieve $O(p^3)$ complexity, we used a translation method based on the rotation-coaxial translation decomposition of an arbitrary translation operators:

$$(\mathbf{E}|\mathbf{F})(\mathbf{t}) = \mathbf{Rot}^{-1}\left(\frac{\mathbf{t}}{t}\right)(\underline{\mathbf{E}|\mathbf{F}})(t)\mathbf{Rot}\left(\frac{\mathbf{t}}{t}\right), \quad t=|\mathbf{t}|, \quad \mathbf{E},\mathbf{F}=\mathbf{S},\mathbf{R}, \tag{58}$$

where $\mathbf{Rot}(\mathbf{t}/t)$ is the rotation transform matrix, which enables one to obtain the expansion coefficients in the reference frame rotated by such way that the z axis of the new reference frame is directed as the unit vector $\mathbf{t}/t$, $(\mathbf{E}|\mathbf{F})(t)$ denotes the coaxial translation matrix that performs $\overline{\text{tran}}$slation along the z axis for distance t and $\mathbf{Rot}^{-1}(\mathbf{t}/t)$ is the backward rotation, which brings the reference frame to its initial orientation. Each of these operations can be performed with complexity $O(p^3)$ using a recursive computation of the matrix elements (Gumerov and Duraiswami, 2003). So, e.g., for the $(\mathbf{S}|\mathbf{R})$ translation of some vector **C**, we first produce $\tilde{\mathbf{C}} = \mathbf{Rot}(\mathbf{t}/t)\mathbf{C}$, then $\mathbf{C}' = (\mathbf{S}|\mathbf{R})(t)\tilde{\mathbf{C}}$, and finally $\hat{\mathbf{C}} = \mathbf{Rot}^{-1}(\mathbf{t}/t)\mathbf{C}'$ for the expense of $O(p^3)$ operations, opposed to $O(p^4)$ operations if we use straightforward multiplication $\hat{\mathbf{C}} = (\mathbf{S}|\mathbf{R})(\mathbf{t})\mathbf{C}$.

1. Rotation transform

In general, an arbitrary rotation transform can be specified by three angles of rotation, e.g., the Euler angles, α_E, β_E, γ_E, or angles α, β, γ related to the Euler angles as $\alpha = \pi - \alpha_E$, $\beta = \beta_E$, and $\gamma = \gamma_E$, which are more convenient, since they are related to the spherical angles (θ_t, φ_t) of the unit vector $\mathbf{t}/t = (\sin\theta_t \cos\varphi_t, \sin\theta_t \sin\varphi_t, \cos\theta_t)$ as $\beta = \theta_t$ and $\alpha = \varphi_t$ (see Fig. 5). The rotation transform of the expansion coefficients is a function of the rotation matrix $Q(\alpha, \beta, \gamma)$. The inverse rotation transform is the same func-

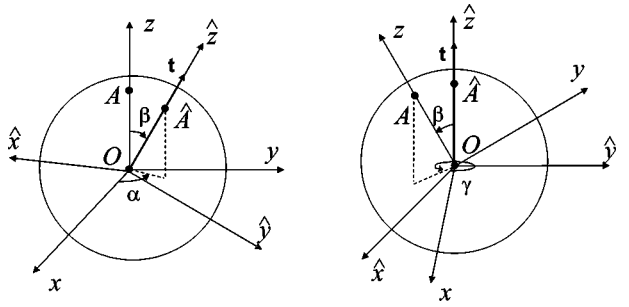

FIG. 5. An illustration of rotation specified by angles α, β, and γ. Angles β and α are the spherical polar angles of the translation vector **t**.

tion from the inverse rotation matrix $Q^{-1}(\alpha,\beta,\gamma)=Q^T(\alpha,\beta,\gamma)=Q(\gamma,\beta,\alpha)$, so we can describe only the forward rotation, since the inverse rotation can be obtained simply by exchanging angles α and γ.

Rotation of the truncated vector **C** with components $\{C_n^{m'}\}$ can be performed according to the following formula:

$$\tilde{C}_n^{m'}=e^{-im'\gamma}\sum_{m=-n}^{n}H_n^{m'm}(\beta)e^{im\alpha}C_n^m,\quad n=0,1,...,p-1,\quad m'=-n,\ldots,n. \tag{59}$$

Here $H_n^{m'm}(\beta)$ are the entries of a real dense matrix that can be computed recursively (Gumerov and Duraiswami, 2003):

$$H_{n-1}^{m',m+1}=\frac{1}{b_n^m}\left\{\frac{1}{2}[b_n^{-m'-1}(1-\cos\beta)H_n^{m'+1,m}-b_n^{m'-1}(1+\cos\beta)H_n^{m'-1,m}]-a_{n-1}^{m'}\sin\beta H_n^{m'm}\right\},$$
$$n=2,3,...,\quad m'=-n+1,...,n-1,\quad m=0,...,n-2, \tag{60}$$

starting with the initial values

$$H_n^{m'0}(\beta)=(-1)^{m'}\sqrt{\frac{(n-|m'|)!}{(n+|m'|)!}}P_n^{|m'|}(\cos\beta),\quad n=0,1,...,\quad m'=-n,\ldots,n. \tag{61}$$

The coefficients a_n^m and b_n^m of the recurrence relation (60) are

$$a_n^m=\begin{cases}\sqrt{\dfrac{(n+1+|m|)(n+1-|m|)}{(2n+1)(2n+3)}}, & n\geqslant|m|,\\ 0, & |m|>n,\end{cases} \tag{62}$$

$$b_n^m=\begin{cases}\sqrt{\dfrac{(n-m-1)(n-m)}{(2n-1)(2n+1)}}, & 0\leqslant m\leqslant n,\\ -\sqrt{\dfrac{(n-m-1)(n-m)}{(2n-1)(2n+1)}}, & -n\leqslant m<0,\\ 0, & |m|>n.\end{cases} \tag{63}$$

The amount of the recursive computations can be reduced using the symmetry relations:

$$H_n^{mm'}(\beta)=H_n^{m'm}(\beta)=H_n^{-m',-m}(\beta),\quad n=0,1,...,\quad m',m=-n,\ldots,n. \tag{64}$$

So computations of the general rotation can be organized as follows. First we compute all rotation coefficients $H_n^{m'm}(\beta)$. This requires $O(p^3)$ operations. Then we perform the multiplication $D_n^m=e^{im\alpha}C_n^m$, $n=0,1,...,p-1$, $m=-n,\ldots,n$. This can be treated as multiplication of vector **C** by a diagonal matrix and requires $O(p^2)$ operations. Then for each subspace of degree n we perform multiplication of the dense $(2n+1)\times(2n+1)$ matrix with the entries $H_n^{m'm}(\beta)$ by vector **D**, and this totals in $O(p^3)$ operations for all subspaces and produces the vector **G**. The last step is multiplication of this vector by the diagonal matrix, to produce the final result: $\tilde{C}_n^{m'}=e^{-im'\gamma}G_n^{m'}$, $n=0,1,...,p-1$, $m'=-n,\ldots,n$. This takes $O(p^2)$ operations.

We note that the decomposition can be simplified by setting $\gamma=0$, since the rotations with angles α and β align the new z axis with direction $\mathbf{t}/t$, while the latter rotation does not change this direction (see Fig. 5). So the forward transform can be performed with the rotation matrix $Q(\varphi_t,\theta_t,0)$ ($\alpha=\varphi_t$, $\beta=\theta_t$, $\gamma=0$) and the inverse with $Q(0,\theta_t,\varphi_t)$.

2. Coaxial translation

Coaxial translations, or translations along the z axis, can also be performed with lower complexity than the general translation, since each subspace of order m is invariant with respect to this type of translation. So if $\hat{\mathbf{C}}=(\underline{\mathbf{E}|\mathbf{F}})(t)\mathbf{C}$, we have

$$\hat{C}_{n'}^m=\sum_{n=|m|}^{p-1}(E|F)_{n'n}^m(t)C_n^m,\quad m=0,\pm1,...,\pm(\min(p,p')-1),\quad n'=0,1,...,p'-1,\quad E,F=S,R. \tag{65}$$

Here $(E|F)_{n'n}^m$ are the entries of matrix $(\mathbf{E}|\mathbf{F})(t)$, which is truncated rectangularly, since it applies to vector **C** of total length p^2 and produces a vector $\hat{\mathbf{C}}$ of total length $(p')^2$. This is due to the algorithm, where the truncation number must change from level to level. Since the truncation numbers p' and p are of the same order, the total complexity of the matrix-vector multiplication (65) is $O(p^3)$ for a given translation matrix. All entries of this matrix can be computed recursively for an expense of $O(p^3)$ operations using the following recursions (Gumerov and Duraiswami, 2003):

To advance with respect to the order n at fixed $m\geqslant0$:

$$a_n^m(E|F)_{n',n+1}^m=a_{n-1}^m(E|F)_{n',n-1}^m-a_{n'}^m(E|F)_{n'+1,n}^m+a_{n'-1}^m(E|F)_{n'-1,n}^m,\quad n=m,m+1,...,\quad E,F=S,R, \tag{66}$$

with the a's given by Eq. (62). For advancement with respect to m:

$$b_{m+1}^{-m-1}(E|F)_{n',m+1}^{m+1}=b_{n'}^{-m-1}(E|F)_{n'-1,m}^m-b_{n'+1}^m(E|F)_{n'+1,m}^m, \tag{67}$$

$$n' = m+1, m+2, \ldots, \quad E,F = S,R,$$

with the b's given by Eq. (63). The recursive procedure starts with the initial values

$$(S|R)^0_{n'0}(t) = (-1)^{n'}\sqrt{2n'+1}\,h_{n'}(kt),$$

$$(R|R)^0_{n'0}(t) = (-1)^{n'}\sqrt{2n'+1}\,j_{n'}(kt). \tag{68}$$

For the Helmholtz equation we have $(S|S)^m_{n'n}(t) = (R|R)^m_{n'n}(t)$, and so only the latter coefficients need be computed. We also note that computational savings can be achieved using the following symmetries of the coaxial translation coefficients:

$$(E|F)^m_{n'n} = (E|F)^{-m}_{n'n} = (E|F)^{|m|}_{n'n} = (-1)^{n+n'}(E|F)^m_{nn'},$$
$$E,F = S,R. \tag{69}$$

G. Use of the FMM for preconditioning in the GMRES

Our computations show that the plain (without preconditioning) GMRES slows down substantially at larger N and for relatively high volume fractions of the spheres (in this case the number of iterations increases proportionally to N). If $N_{\text{iter}} = O(N)$ then a method that requires $O(N \log N)$ per matrix-vector multiplication will require $O(N^2 \log N)$ operations to solve the problem. We found that this drawback can be fixed in many cases by the use of properly designed preconditioners. The GMRES with the right preconditioner $\mathbf{M}^{-1}$ solves the problem

$$\mathbf{L}\mathbf{M}^{-1}(\mathbf{M}\mathbf{A}) = \mathbf{E}, \tag{70}$$

which is formally equivalent to the original problem (23) for arbitrary invertible matrix $\mathbf{M}$. If solution of the system $\mathbf{M}\mathbf{A}=\mathbf{F}$ for an arbitrary input $\mathbf{F}$ can be obtained faster than solution of the original system $\mathbf{L}\mathbf{A}=\mathbf{F}$, and $\mathbf{M}$ is a good approximation of $\mathbf{L}$ ($\mathbf{M}\approx\mathbf{L}$), then one can expect a substantial reduction in the number of iterations.

The FMM provides a good tool for building a preconditioner (for the discussion of preconditioning see Kelly, 1995; Saad, 2003). The preconditioners that can be constructed are based on decompositions of the dense $(\mathbf{S}|\mathbf{R})$ matrix in Eq. (28):

$$(\mathbf{S}|\mathbf{R}) = (\mathbf{S}|\mathbf{R})_{\text{near}} + (\mathbf{S}|\mathbf{R})_{\text{far}}, \quad \mathbf{M}_{\text{sparse}} = \mathbf{T}^{-1} - (\mathbf{S}|\mathbf{R})_{\text{near}},$$

$$\mathbf{M}_{\text{dense}} = \mathbf{T}^{-1} - (\mathbf{S}|\mathbf{R})_{\text{far}}, \tag{71}$$

where $(\mathbf{S}|\mathbf{R})_{\text{near}}$ is a sparse matrix, which includes only interactions between the scatterers located in the same neighborhood (say at the maximum level of space subdivision), and $(\mathbf{S}|\mathbf{R})_{\text{far}}$ is the matrix, which includes farfield interactions. This decomposition, in fact, is decomposition (35) in terms of the resulting vector $\mathbf{B}$. The matrix-vector products $\mathbf{M}_{\text{sparse}}\mathbf{A}$ or $\mathbf{M}_{\text{dense}}\mathbf{A}$ involving preconditioners $\mathbf{M}_{\text{sparse}}$ and $\mathbf{M}_{\text{dense}}$ then can be computed faster than $\mathbf{L}\mathbf{A}$, since only part of the FMM operations are needed to perform the computations. At first look, it seems that it is more reasonable to use $\mathbf{M}_{\text{sparse}}$ as the preconditioner, since presumably matrix-vector multiplication in this case should be cheaper. However, there are two reasons, both working in the same direction, why the use of $\mathbf{M}_{\text{dense}}$ may make more sense.

The first reason is based on the efficiency of the preconditioner in terms of the process convergence. Despite the fact that the distance between the neighbor scatterers is smaller and the interaction between any pair of neighbors is stronger than between the remote particles, the number of neighbors is also substantially smaller. Since this interaction decays as r^{-1}, while the number of particles in the farfield increases as r^3 (for a uniform distribution) the effect of the farfield on the given scatterer dominates for larger domain sizes and a larger number of scatterers. Most computational work then is to iterate the solution for a proper determination of the farfield, and that is what the unpreconditioned method does.

The second reason is a feature of the FMM that appears to have been used for the first time here. It is based on the efficiency of the preconditioner in terms of the speed of matrix-vector multiplication. It may seem paradoxical but in the FMM as described above the computation of $(\mathbf{S}|\mathbf{R})_{\text{far}}\mathbf{A}$ can be much faster than the computation of $(\mathbf{S}|\mathbf{R})_{\text{near}}\mathbf{A}$. This happens due to limitations of type (31) on the maximum level of space subdivision and takes place for a relatively high volume fraction of scatterers [for low volume fractions $(\mathbf{S}|\mathbf{R})_{\text{near}}\mathbf{A}$ can be computed faster]. Indeed if $l_{\max}$ is small enough, then the most computational work is spent for direct computations of matrix-vector products $\mathbf{B}_{\text{near}} = (\mathbf{S}|\mathbf{R})_{\text{near}}\mathbf{A}$ [for $l_{\max}=1$ we have $(\mathbf{S}|\mathbf{R})_{\text{near}} = (\mathbf{S}|\mathbf{R})$ and need to multiply the matrix by vector directly for cost $O(N^2)$]. An increase of $l_{\max}$ reduces the number of direct matrix-vector products, while increasing the total number of translations. There exist some optimum $l^{\text{opt}}_{\max}$, where the costs of translations and direct computations is balanced. It appears that for high volume fractions of scatterers $l^{(\text{opt})}_{\max} > l_{\max}$, where $l_{\max}$ is limited by condition (31) (we checked this numerically for some spatially uniform random distributions of the scatterers), and so the use of $\mathbf{M}_{\text{dense}}$ is preferable.

Finally, we note that we computed the matrix-vector product $\mathbf{A} = \mathbf{M}^{-1}\mathbf{F}$ by solving $\mathbf{M}\mathbf{A}=\mathbf{F}$ using the unpreconditioned GMRES, which introduced an internal iteration loop. As a convergence criterion for this internal process we imposed the error of iteration much larger than the error for an external loop (this is possible, since the preconditioner can be computed roughly). This type of iterative scheme produces poor results if a regular GMRES is used, due to the nonlinear dependence of $\mathbf{A}$ on $\mathbf{F}$ in this process. It is also well known that this drawback can be fixed by the use of flexible GMRES, which we do. For details refer to Saad (1993).

VI. NUMERICAL RESULTS AND DISCUSSION

A. Test problems computed

The multiple scattering problem even with spherical scatterers is a multiparametric problem with many degrees of freedom. In the tests we selected a few typical types of spatial distributions: uniformly random, periodic (spheres in a grid), randomly periodic, where some random pattern is repeated several times in a cubic mesh, and uniformly random with some limitations on the interparticle distances (e.g., that the ratio of the minimum distance between the sphere centers to the sphere radius, $d_{\min}/a$, is some prescribed number). The

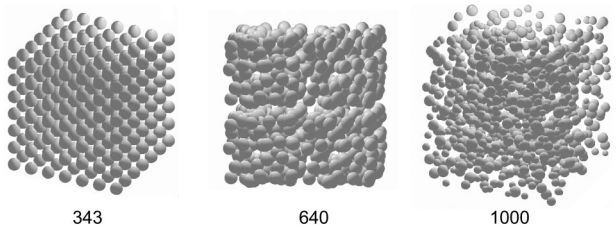

FIG. 6. Examples of distributions of N spheres used in computations: periodic, randomly periodic, and random.

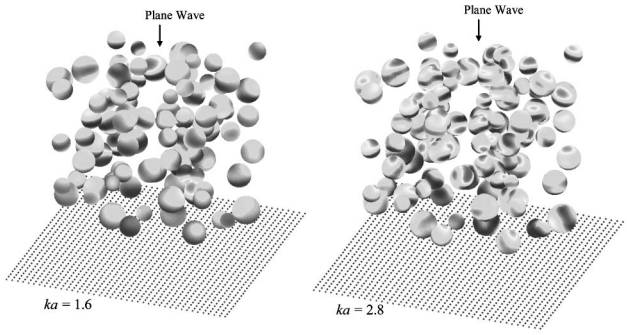

FIG. 7. Examples of the computation of the surface potential for 100 spheres exposed to a plane wave directed as shown by the arrows.

latter type of distribution enables computations with high accuracy (which depends on $d_{\min}/a$, as discussed above). We also performed computations for monodisperse (all spheres of the same size) and polydisperse systems (see Fig. 6). In the latter case the radii of the spheres were distributed between some $a_{\min}$ and $a_{\max}$ (we used uniformly random distributions, while other situations are possible, depending on a particular physical problem). The number of spheres was varied in range $N=[10,10\,000]$. This also depends on ka, which was varied in range $0.1<ka<5$, and the volume fraction of the spheres in the computational domain, α:

$$\alpha=\frac{4\pi N a^3}{3D_0^3}, \quad a^3=\sum_{q=1}^{N} a_q^3. \tag{72}$$

For larger ka and smaller α we used smaller number N to stay within the range $kD_0<100$, according to the equation

$$kD_0=\left(\frac{4\pi N}{3\alpha}\right)^{1/3} ka. \tag{73}$$

Potentially larger kD_0's are possible; however, some loss of precision was observed at larger kD_0, which may be related to the number of bits representing float numbers and the growth of the cut-off errors.

We also varied the boundary admittances σ_q of the scatterers. Despite the fact that the procedure allows computations with different σ_q's for each scatterer, we did not conduct systematic tests of this case and in all computations we assumed that all admittances are the same $\sigma_q=\sigma$, $q=1,...,N$.

B. Field visualization

Once computations of the expansion coefficients $\{\mathbf{A}^{(q)}\}$ are performed, the problem is how to determine the surface and spatial distributions of the potential and the surface distributions of its normal derivative. A computation of the surface distributions is a relatively easy task, since we have (GD02),

$$\psi|_{S_q}=\frac{1}{ika_q^2}\sum_{n=0}^{p-1}\sum_{m=-n}^{n}\frac{A_n^{(q)m}Y_n^m(\theta_q,\varphi_q)}{kj_n'(ka_q)+i\sigma_q j_n(ka_q)}, \tag{74}$$

$$\left.\frac{\partial\psi}{\partial n}\right|_{S_q}=-\frac{\sigma_q}{ka_q^2}\sum_{n=0}^{p-1}\sum_{m=-n}^{n}\frac{A_n^{(q)m}Y_n^m(\theta_q,\varphi_q)}{kj_n'(ka_q)+i\sigma_q j_n(ka_q)}$$
$$=-i\sigma_q\psi|_{S_q}. \tag{75}$$

An example of surface potential visualization for the case of 100 spheres is shown in Fig. 7.

A computation of the potential at M spatial locations $\mathbf{y}_m$, $m=1,...,M$ can be a computationally more expensive task than the solution of the problem itself, if this is performed in a straightforward way. The spatial visualization, however, can be performed as fast as the solution and with the same accuracy, if the FMM is applied to this task. Two major modifications of the algorithm are needed in this case. First, we separate the set of N scatterer centers from the set of M evaluation points. The octree-based space partitioning is applied to the new data structure. As soon as the expansion coefficients $\mathbf{A}^{(q)}$, $q=1,...,N$ are known, the upward pass then is the same as for solution of the scattering problem, while in the downward pass the process goes over the hierarchy of the evaluation points [see the separation of data hierarchies discussed in Gumerov *et al.*, (2003)]. At the end of the downward pass we obtain the expansion coefficients $\mathbf{D}^{(n,l_{\max})}$ for each target box (the box containing the evaluation points). Then, as the final summation step, we compute the potential for all evaluation points as

$$\psi(\mathbf{y}_m)=\psi_{\text{in}}(\mathbf{y}_m)+\mathbf{D}^{(n,l_{\max})}\cdot\mathbf{R}(\mathbf{y}_m-\mathbf{r}_*^{(n,l_{\max})})$$
$$+\sum_{\mathbf{r}_q'\in E_2(n,l_{\max})}\mathbf{A}^{(q)}\cdot\mathbf{S}(\mathbf{y}_m-\mathbf{r}_q'),$$
$$\forall\,\mathbf{y}_m\in E_1(n,l_{\max}), \quad m=1,...,M. \tag{76}$$

Here the first term on the right-hand side is the known potential of the incident field at the receiver locations, the second term is the potential of the field scattered by the scatterers located outside the neighborhood of the target box, and the third term is a field scattered by the scatterers located in the neighborhood of the receiver and found by direct evaluation. The complexity of this procedure for the $O(p^3)$ translation method is of type $O((N+M)\log N)$ if the same $l_{\max}$ is used for the space imaging method as for the solution of the problem. If there are many imaging points in a target box, finer space partitioning can be used to reduce the complexity, and the optimum number of levels can be found experimentally or based on some theory applicable for the FMM (Gumerov *et al.*, 2003).

Figure 8 illustrates the "speckle patterns" on the image plane shown in Fig. 7 by blue dots. The solution is obtained using the FMM both for an accelerated iterative solution of

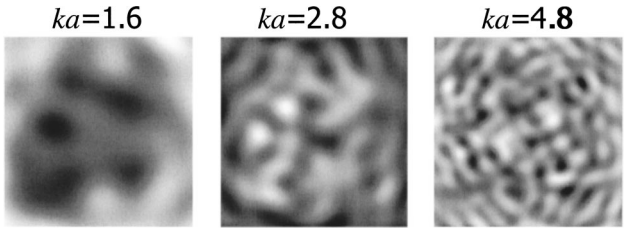

FIG. 8. Speckle patterns on the imaging plane computed using the FMM for scattering of plane waves of different wavelengths from 100 scatterers (the geometry and the imaging plane are shown in Fig. 7).

the linear system and for imaging of the field as described. The images are computed for monochromatic fields of different frequencies. These pictures are frames of a movie that animates the wave propagation in time, by plotting $\mathrm{Re}\{\psi(\mathbf{r})e^{-i\omega t}\}$ for different t. A similar figure (Fig. 9) illustrates the ''speckle patterns'' for the case of 10 000 equal spheres ($a=1$) with centers that are randomly distributed inside a cube $80\times80\times80$ ($d_{\min}=2.5$).

C. *A posteriori* error evaluation

For these tests we used Eq. (51) to obtain the truncation number where we varied p_0, and Eqs. (54) and (55) for the FMM procedure, where ϵ was specified to be the same as for the convergence of the iterative process. After the iterative process (GMRES) was terminated, we computed the potential at M sampling points according to Eq. (74) and the relative errors in boundary conditions using (53). The spheres were distributed randomly inside a cubic box with the restriction that the distance between the sphere centers exceeds some prescribed $d_{\min}$. Test were made for the incident wave $\psi_{\mathrm{in}}(\mathbf{r})=e^{i\mathbf{k}\cdot\mathbf{r}}$.

An example of the computed surface error is shown in Fig. 10. This figure illustrates the behavior of $|\psi||_{S_q}(\mathbf{y}_m)$ and $\Delta_{bc}(\mathbf{y}_m)$ for $M=3200$ sampling points allocated on the surfaces of 100 equal size sound-hard spheres for $p=11$ ($ka=1$, $kD_0\approx30$, $\sigma=0$, $\alpha=0.042$, $d_{\min}/a=3$, $l_{\max}=3$, $\epsilon=10^{-10}$). It is seen that the maximum absolute error of computations in this case is less than 10^{-4}, while the average error of computations is of the order of 10^{-6}.

The parameter $d_{\min}/a$ has a substantial effect on the accuracy. Figure 11 illustrates this effect for the same settings as for 10, where the truncation number and $d_{\min}/a$ were varied. The relative error $\epsilon^{(bc)}$ defined by Eq. (53), that also can

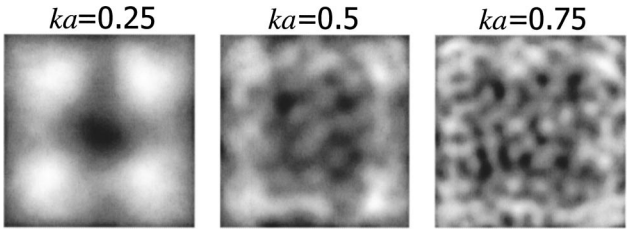

FIG. 9. Speckle patterns on the imaging plane computed using the FMM for scattering of plane waves of different wavelength from 10 000 spheres of size $a=1$ randomly distributed inside a cube $80\times80\times80$. The image plane is located at $z=82$ (assuming that the computational domain is between $z=-1$ and $z=81$ and the plane wave propagates in the positive direction).

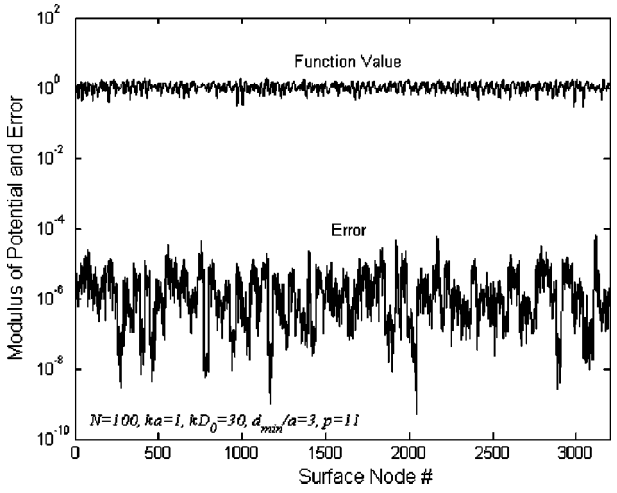

FIG. 10. The modulus of the potential and the absolute error in boundary conditions obtained *a posteriori* as functions on the surface node index. The surface of each of 100 spheres was sampled by 32 points.

be assigned as the relative error in the ''infinity'' norm L_∞, is much larger (about one order of magnitude) than the average, or L_2-norm error, $\epsilon_2^{(bc)}$, defined as

$$\epsilon_2^{(bc)}=\frac{1}{M}\left\{\sum_{m=1}^{M}[\epsilon_m^{(bc)}]^2\right\}^{1/2}, \tag{77}$$

with $\epsilon_m^{(bc)}$ specified in Eq. (53). It is seen that even for the case when the spheres may touch ($d_{\min}/a=2$), computations can be performed with relatively small truncation numbers if an accuracy $\epsilon^{(bc)}$ of the order of a few percent is acceptable (that might be sufficient for comparisons with experiments, field imaging, etc.). For computations with high precision, the truncation numbers should be increased, which may substantially slow down the computation process. One of the methods to treat this drawback is to introduce truncation numbers p_q for each scatterer, $q=1,...,N$, which should depend on the distance from the qth sphere to its closest neighbor sphere. In the present study, however, we did not perform

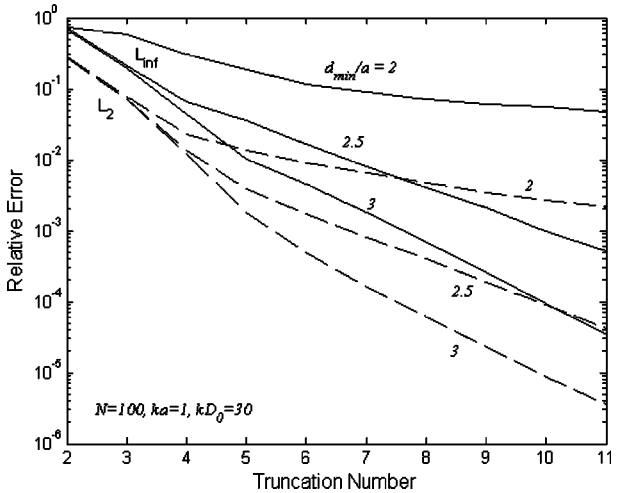

FIG. 11. Dependencies of the relative errors in the infinite (solid lines) and quadratic (dashed lines) norms on the truncation number p for the same parameters as shown in Fig. 10. The errors are computed for random distributions with different ratios $d_{\min}/a$ shown near the curves.

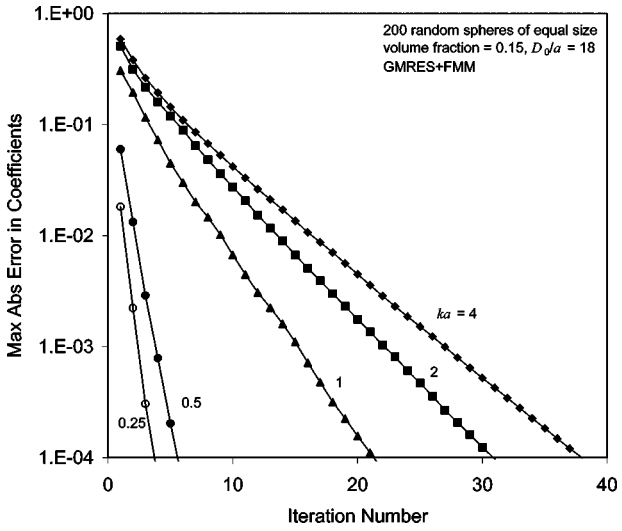

FIG. 12. Convergence of the unpreconditioned GMRES at different dimensionless wave numbers ka shown near the curves.

modifications, since our goal was to develop and test the base algorithm.

D. Convergence

Several factors may affect the rate of convergence of the iterative method and more or less a complete study involves the investigation of the multiparametric space. In the present tests we usually fixed all parameters for the case and varied one or two parameters to see their effect on the convergence rate and accuracy of computations. Figure 12 shows the effect of the frequency on the convergence of unpreconditioned GMRES. For the case illustrated, 200 equal size sound-hard spheres with random distribution of their centers were generated as described above ($d_{\min}/a=2.3$). The truncation numbers were selected according to Eq. (51) with a constant $p_0=10$ for all cases, while the FMM truncation numbers were determined according to Eq. (54) with $\epsilon=10^{-4}$. It is seen that in this case the number of iterations to achieve specified accuracy increases with ka. An *a posteriori* error check for the boundary conditions at 6400 points shows that for this case the error $\epsilon^{(bc)}$ defined by Eq. (53) does not exceed 5×10^{-3} for all cases, while $\epsilon_2^{(bc)}$ defined by Eq. (77) is about 1 order of magnitude smaller. We found that the iteration process for higher frequencies ($ka\gtrsim5$, $kD_0\gtrsim100$) diverges, and special methods for treatment of higher frequencies are required. Several methods can be tried in this case, such as using preconditioners based on high-frequency asymptotic expansions of the system matrix, and some relaxation methods, where, e.g., the impedance of the spheres, σ, can be gradually adjusted during the iteration process. Indeed, we did some preliminary computations with fixed $ka=4$ and varying σ and found that, say for $\sigma/k\sim0.1$, the number of iterations to achieve the same accuracy drops by a factor of 2.

Properly designed preconditioners can substantially reduce the computation time to obtain a solution of specified accuracy. Some results of the use of GMRES and FGMRES with the right dense preconditioner $\mathbf{M}_{\text{dense}}$ [see Eq. (71)] is shown in Table I. This table shows computational results for

TABLE I. Performance of the FMM accelerated GMRES/FGMRES. $N=10\,000$. Number of complex unknowns$=2.25\times10^6$.

Preconditioner	No. external iterations	No. internal iterations	CPU time (s)
No preconditioner	58	0	8340
Right dense, $\epsilon_{\text{pre}}=0.1$	11	87	3460
Right dense, $\epsilon_{\text{pre}}=0.01$	10	165	4525

10 000 sound hard spheres of equal size with a randomly periodic distribution (blocks of 80 spheres with random distribution of centers, $d_{\min}/a=2$, $\alpha=0.2$, were repeated 125 times to occupy a larger cube). Here $D_0/a=60$ and $ka=0.5$, $l_{\max}=4$, $\epsilon=10^{-4}$, $p=7$, and the CPU time was measured for 3.2 MHz dual Intel Xeon processor (3.5 GB RAM, 25% CPU resource allocation for a task). The table shows that the number of iterations for the external loop can be drastically reduced due to the use of a preconditioner. The price to pay for this is the internal iterative loop, which uses also GMRES to obtain a solution of the equation $\mathbf{M}_{\text{dense}}\mathbf{A}=\mathbf{F}$. However, for the present case matrix-vector multiplication $\mathbf{M}_{\text{dense}}\mathbf{A}$ was seven times faster than performing multiplication $\mathbf{LA}$ (both using the FMM). This resulted in a decrease of the overall computational time. A solution of equation $\mathbf{M}_{\text{dense}}\mathbf{A}=\mathbf{F}$ can be performed with much less accuracy, ϵ_{pre} (shown in the first column of the table), than the accuracy required for the external iterative process. This can be a subject for optimization, since the increase of the accuracy for internal iterations reduces the number of external iterations and increases the number of the internal iterations. We also need to mention that the efficiency of preconditioners depend on several other parameters, including wave number, number of scatterers, surface admittance, volume fraction, etc. (See Table I)

E. Performance study

To determine the dependence of the CPU time required for a solution of the problem, and to check the consistency of the actual results with the theoretical predictions, we conducted a performance study. All computations were made in double precision complex arithmetic on a desktop PC (3.2 MHz dual Intel Xeon processor, 3.5 GB RAM, 25% CPU resource allocated for a task). As a test distribution we used randomly periodic distributions of equal size sound hard spheres (blocks of 80 spheres with random distribution of centers, $d_{\min}/a=2$, were repeated m^3 times to occupy a larger cube, $m=1,...,5$; an example for $m=2$, $N=640$ is shown in Fig. 6). Since the volume fraction and the wave number in the tests were fixed ($\alpha=0.2$, $ka=0.5$) the increase in the number of spheres also means the increase of the size of the computational domain [see Eq. (73)].

We found that to reduce the CPU time for the present case, one should select the computational domain size larger than the size of the box, which encloses all the spheres. The size of the computational domain can be determined based on $l_{\max}$ according Eq. (33) as

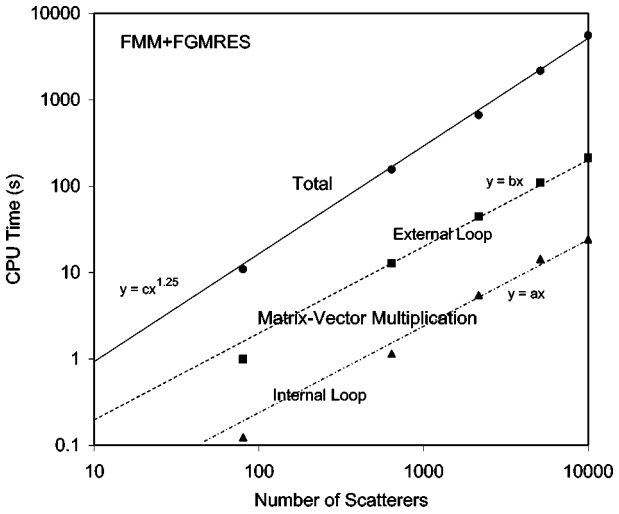

FIG. 13. Dependences of the CPU time (Intel Xeon 3.2 GHz, 3.5 Gb RAM) on the number of scatterers ($ka=0.5$, $p=15$, $\epsilon=10^{-4}$) for randomly-periodic distribution of sound-hard spheres of equal size (see Fig. 6). The triangles and squares show the CPU time required for matrix-vector multiplication using the FMM for the preconditioner and full matrix, respectively. The disks show the total CPU time for the execution of the algorithm. The lines show the interpolation of data.

$$D_0=\frac{2\delta_{\min}}{4-(1+\delta_{\min})\sqrt{3}}2^{l_{\max}}a_{\max}. \tag{78}$$

Setting here $l_{\max}=2,3,...$, we can determine a discrete set of D_0. For computations we selected the minimum of D_0 from this set, which encloses all the spheres. Although $\delta_{\min}$ here should be larger than 1, we found with the *a posteriori* error check that $\delta_{\min}=1$ provides stable and accurate results in this case. Note that for performance tests we accepted relative errors $\epsilon^{(bc)}$ of about 2% (the errors $\epsilon_2^{(bc)}$ were one order of magnitude smaller). To provide this order of errors we set $\epsilon=10^{-4}$ for the global iteration convergence, while the error for the preconditioner was set to $\epsilon_{\text{pre}}=0.2$. In all computations we used a truncation number of $p=15$. This substantially exceeds $p_{l_{\max}}\sim 8$, and the choice of p was dictated by a desire to compute accurately the case of touching spheres. Since the excessive value $p=15$ is due only to the influence of the neighbor spheres, for each sphere we took the contribution of the neighbors with $d/a<1.3$ into harmonics of degree $n=8,...,15$, while we neglected the effect of other scatterers on these harmonics (see the discussion at the end of Sec. V D). An *a posteriori* error check showed that the relative errors specified above were achieved.

Figure 13 shows the measurements of the CPU time for various operations of the algorithm based on the FGMRES with a right preconditioner. It is seen that the computation time scales almost linearly for a single matrix-vector multiplication in the internal or external loop using the FMM. This agrees well with the theoretical predictions of complexity $O(N\log N)$. Due to the growth of the number of iterations both in the internal and external loops with N, the total CPU time scales as $O(N^{1.25})$. This shows that some average number of internal–external iterations, N_{iter}, is proportional in the present case to $N^{0.25}$ or so. As it was discussed previously, an optimum can be sought by varying ϵ_{pre}, and possibly, ϵ, to perform better, while we kept these parameters for the illustration case fixed. Note that for large N and unpreconditioned GMRES we found that the number of iterations N_{iter} grows proportionally to N for $N\gtrsim 2000$, which substantially reduces the efficiency of the algorithm.

It is also noteworthy that even for $N=80$ the size of the complex system matrix $\mathbf{L}$ is $Np^2\times Np^2=18\,000\times 18\,000$, which would require several hours to solve the problem directly, while the present method requires only 10 s for this operation. We also found that a solution of this problem using GMRES without preconditioners and the FMM for matrix-vector multiplication takes about 75 s of CPU time for the same machine. Cases with larger N were not even computable due to memory limitations.

VII. CONCLUSIONS

We have developed and tested a procedure for a solution of the acoustic scattering problems for the case of clusters consisting of a relatively large number of spherical scatterers of various radii and impedances arbitrarily located in three-dimensional space. This procedure uses a multipole re-expansion technique, the fast multipole method, and iteration algorithms, such as GMRES with possible preconditioners and is accelerated utilizing the FMM. We developed and tested a technique for *a posteriori* error control, investigated convergence, and performance of the method in a certain range of parameters and found that this technique can be an efficient, accurate, and powerful tool for solution of such multiple scattering problems.

While the method is developed and tested for spherical scatterers, it can be naturally extended for the computation of scattering from objects of an arbitrary shape, as soon as the T matrices for the single scatterers are known analytically or precomputed numerically. Several research issues for further improvement of the method remain open, e.g., the problem of computations for very high frequencies or large domain sizes, $kD_0\gtrsim 100$.

ACKNOWLEDGMENTS

We would like to gratefully acknowledge the support of NSF awards No. 0219681 and No. 0086075. We would also like to thank Professor Howard Elman and Professor Dianne O'Leary for discussions and guidance related to iterative methods used in the present study. We would also like to thank Professor Rajarshi Roy for suggesting the ''speckle pattern'' problem.

Nigmatulin, R. I. (**1990**). *Dynamics of Multiphase Media* (Hemisphere, Washington, DC).

Caflisch, R., Miksis, M., Papanicolaou, G. C., and Ting, L. (**1985**). ''Effective equations for wave propagation in bubbly liquids,'' J. Fluid Mech. **153**, 259–273.

Gumerov, N. A., Ivandaev, A. I., and Nigmatulin, R. I. (**1988**). ''Sound waves in monodisperse gas-particle or vapor-droplet mixtures,'' J. Fluid Mech. **193**, 53–74.

Duraiswami, R., and Prosperetti, A. (**1995**). ''Linear pressure waves in fogs,'' J. Fluid Mech. **299**, 187–215.

Waterman, P. C., and Truell, R. (**1961**). ''Multiple scattering of waves,'' J. Math. Phys. **2**, 512–537.

Peterson, B., and Strom, A. (**1974**). ''Matrix formulation of acoustic scattering from an arbitrary number of scatterers,'' J. Acoust. Soc. Am. **56**, 771–780.
Varadan, V. K., and Varadan, V. V. (**1980**). *Acoustic, Electromagnetic and Elastic Wave Scattering: Focus on the T-Matrix Approach* (Pergamon, New York).
Wang, Y. M., and Chew, W. C. (**1993**). ''A recursive T-matrix approach for the solution of electromagnetic scattering by many spheres,'' IEEE Trans. Antennas Propag. **41**, 1633–1639.
Mishchenko, M. I., Travis, L. D., and Mackowski, D. W. (**1996**). ''T-matrix computations of light scattering by nonspherical particles: a review,'' J. Quant. Spectrosc. Radiat. Transf. **55**, 535–575.
Koc, S., and Chew, W. C. (**1998**). ''Calculation of acoustical scattering from a cluster of scatterers,'' J. Acoust. Soc. Am. **103**, 721–734.
Gumerov, N. A., and Duraiswami, R. (**2002**). ''Computation of scattering from *N* spheres using multipole reexpansion,'' J. Acoust. Soc. Am. **112**, 2688–2701.
Ong, E. T., Heow, P. L., and Kian, M. L. (**2004**). ''A fast Fourier transform on multipoles (FFTM) algorithm for solving Helmholtz equation in acoustic analysis,'' J. Acoust. Soc. Am. **116**, 1362–1371.
Greengard, L., and Rokhlin, V. (**1987**). ''A fast algorithm for particle simulations,'' J. Comput. Phys. **73**, 325–348.
Sangani, A. S., and Mo, G. (**1996**). ''An $O(N)$ algorithm for Stokes and Laplace interactions of particles,'' Phys. Fluids **8**, 1990–2010.
Rokhlin, V. (**1993**). ''Diagonal forms of translation operators for the Helmholtz equation in three dimensions,'' Appl. Comput. Harmon. Anal. **1**, 82–93.
Chew, W. C., Jin J.-M., Michielssen, E., and Song, J. (**2001**). *Fast and Efficient Algorithms in Computational Electromagnetics* (Artech House, Boston).
Darve, E. (**2000a**). ''The fast multipole method: numerical implementation,'' J. Comput. Phys. **160**, 195–240.
Gumerov, N. A., and Duraiswami, R. (**2003**). ''Recursions for the computation of multipole translation and rotation coefficients for the 3-D Helmholtz equation,'' SIAM (Soc. Ind. Appl. Math.) J. Sci. Stat. Comput. **25**, 1344–1381.
Saad, Y. (**2003**). *Iterative Methods for Sparse Linear Systems*, 2nd ed. (SIAM, Philadelpha).
Kelly, C. T. (**1995**). *Iterative Methods for Linear and Nonlinear Equations* (SIAM, Philadelphia).
Greengard, L. (**1988**). *The Rapid Evaluation of Potential Fields in Particle Systems* (MIT Press, Cambridge, MA).
Gumerov, N. A., Duraiswami, R., and Borovikov, E. A. (**2003**). ''Data Structures, Optimal Choice of Parameters, and Complexity Results for Generalized Multilevel Fast Multipole Methods in *d* Dimensions,'' University of Maryland Institute for Advanced Computer Studies Technical Report UMIACS-TR-#2003-28; also CS-TR-#4458. (Available at http://www.cs.umd.edu/Library/TRs/CS-TR-4458/CS-TR-4458.pdf.)
Koc, S., Song, J., and Chew, W. C. (**1999**). ''Error analysis for the numerical evaluation of the diagonal forms of the scalar spherical addition theorem,'' SIAM (Soc. Ind. Appl. Math.) J. Numer. Anal. **36**, 906–921.
Darve, E. (**2000b**). ''The fast multipole method I: error analysis and asymptotic complexity,'' SIAM (Soc. Ind. Appl. Math.) J. Numer. Anal. **38**, 98–128.
Saad, Y. (**1993**). ''A flexible inner-outer preconditioned GMRES algorithm,'' SIAM J. Sci. Comput. (USA) **14**, 461–469.